A volcano transition in a solvable model of oscillator glass

Bertrand Ottino-Löffler & Steve Strogatz

05/21/19

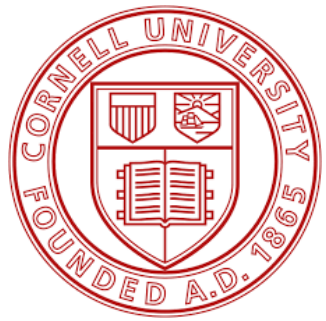

Outline

Oscillators?

Oscillator ingredients

- Each oscillator has a **phase** θ.
- Each oscillator has a **natural frequency** ω.
- Oscillators **couple** to one another.
- There is a tunable **coupling strength** J between oscillators.

Main dynamics

$$\dot{\theta}_j = \omega_j + \sum_{k=1}^{N} J_{jk} \sin\left(\theta_k - \theta_j\right) \text{ for } j = 1, \ldots, N. \tag{1}$$

Background: glass?

Background: what is a glass?

- Slow.
- Messy.
- Complicated.
- Frustrated.

Background: what is a glass?

- Slow, non-exponential/algebraic decay of chosen order parameter to steady states.
- Substantial lack of long-range order or symmetry.
- Significant redundancy in the set of possible ground microstates that all carry similar macroscopic behavior.
- Frustrated.

What does frustration look like?

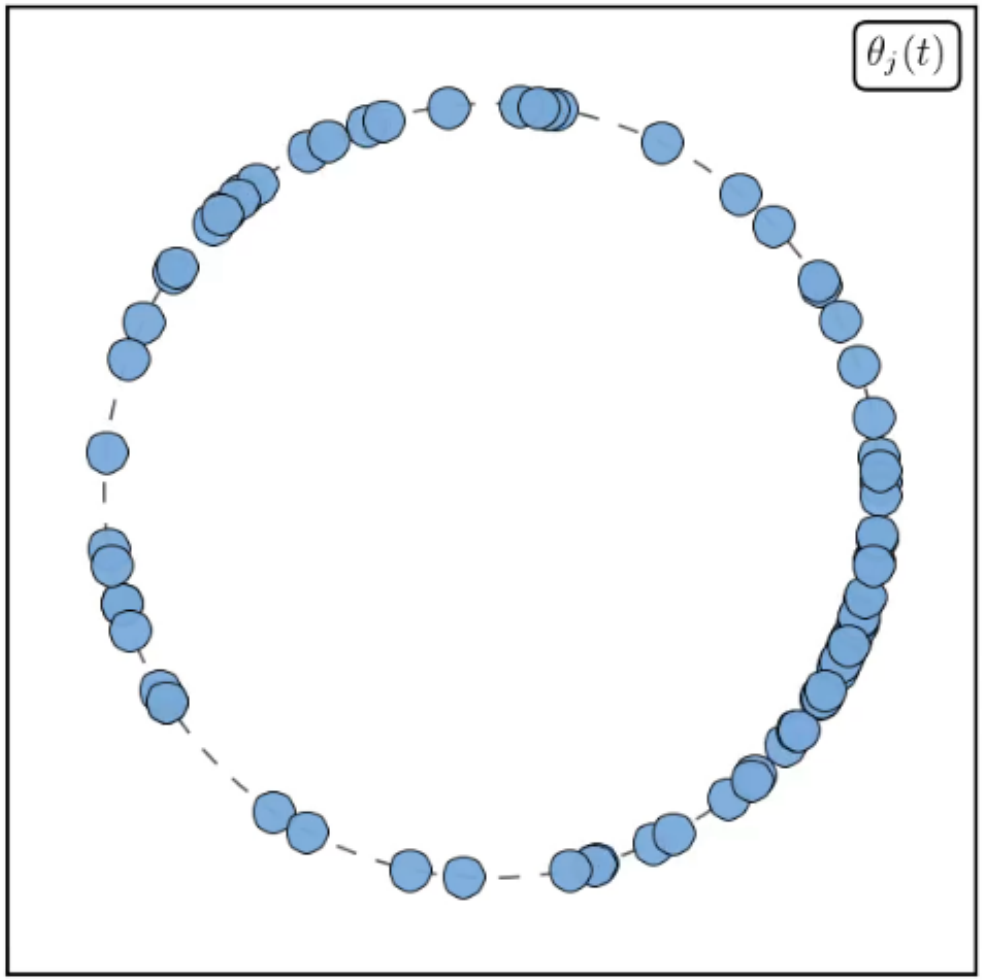

Figure: Phase Video Caption

Can oscillators make a “true” glass?

It's complicated.

PHYSICAL REVIEW E VOLUME 61, NUMBER 2 FEBRUARY 2000

Self-averaging of an order parameter in randomly coupled limit-cycle oscillators

J. C. Stiller
Institut für Biologie III, Universität Freiburg, and AG Hirnforschung, Hansastrasse 9a, D-79104 Freiburg, Germany

G. Radons*
Fraunhofer Institut für Produktionstechnik und Automatisierung (FhG-IPA), Nobelstrasse 12, D-70569 Stuttgart, Germany and Fakultät Physik, Universität Stuttgart, D-70049 Stuttgart, Germany

(Received 11 August 1999)

In our recent paper [Phys. Rev. E **58**, 1789 (1998)] we found notable deviations from a power-law decay for the ''magnetization'' of a system of coupled phase oscillators with random interactions claimed by Daido in Phys. Rev. Lett. **68**, 1072 (1992). For another long-time property, the Lyaponov exponent, we found that his numerical procedure showed strong time discretization effects and we suspected a similar effect for the algebraic decay. In the Comment to our paper [preceding paper, Phys. Rev. E **61**, 2145 (2000)] Daido made clear that the power law behavior was only claimed for the sample averaged magnetization $[Z]$ and he presented new, more accurate numerical results which provide evidence for a power-law decay of this quantity. Our results, however, were obtained for Z itself and not for $[Z]$. In addition, we have taken the intrinsic oscillator frequencies as Gaussian random variables, while Daido in his new and apparently also in his earlier simulations used a deterministic approximation to the Gaussian distribution. Due to the differences in the observed quantity and the model assumptions our and Daido's results may be compatible.

PACS number(s): 05.45.−a

The investigation of interacting biological oscillators was introduced by Winfree [1] several decades ago. Building on Winfree's idea of a phase description, Kuramoto introduced a simple model of interacting phase oscillators [2–5], which could be solved analytically in the limit of $N \to \infty$ coupled oscillators. The dynamics of the phases of the oscillators are described by coupled first order differential equations:

noting the interaction strength. The frequencies ω_j are distributed according to a Gaussian distribution function $f(\omega) = \exp(-\omega^2/2)/\sqrt{2\pi}$.

A continuous distribution function $f(\omega)$ is only well-defined for $N \to \infty$ or for random variables ω_j. Although not stated in [7], in his numerical calculations (with finite N) Daido, in contrast to us [10], used nonrandom frequencies [see Eq. (3) in his comment [11]].

Daido investigated the decay of $Z(t)$ from the initial con-

It's complicated.

PHYSICAL REVIEW E VOLUME 61, NUMBER 2 FEBRUARY 2000

Algebraic relaxation of an order parameter in randomly coupled limit-cycle oscillators

Hiroaki Daido
Department of Physics, Faculty of Engineering, Kyushu Institute of Technology, Kitakyushu 804-8550, Japan
(Received 28 December 1998)

In their recent paper [Phys. Rev. E **58**, 1789 (1998)], Stiller and Radons (SR) study, following our earlier work [Phys. Rev. Lett. **68**, 1073 (1992)], the behavior of globally and randomly coupled phase oscillators with distributed intrinsic frequencies. They claim that their simulation results do not confirm the power-law behavior of an order parameter found numerically by the author, attributing its cause to the poor precision of the author's integration scheme. Here demonstrated is that the power law survives even for a scheme better than SR's, provided that finite-size effects are properly taken into account, as was done in our previous work.

PACS number(s): 05.45.−a, 87.10.+e, 02.50.−r, 05.40.−a

The behavior of large populations of coupled nonlinear oscillators is now one of the central subjects in nonlinear dynamics [1–3]. Although it is usually studied for the case of nonrandom interactions, the architecture of coupling in any kind of real coupled-oscillator systems should involve more or less quenched disorder. If such disorder is weak enough, then it will not cause any significant change in the system's behavior. However, one may expect the emergence of qualitatively new features when randomness in coupling is not decoratively feeble. For example, many biological and physiological oscillator systems, including the brain, might be examples of such a case [1,4]. It is therefore an important and interesting subject to examine the behavior of randomly coupled oscillators. From this point of view, the author started investigations into pools of randomly coupled limit-cycle oscillators more than a decade ago [5] and later proposed a model of ''oscillator glass'' [6],

$$\dot{\theta}_i = \omega_i + \frac{J}{N}\sum^{N}$$

when J exceeds J_c, a threshold value, where $[Z(t)]$ stands for an average of $Z(t)$ over a number of different realizations of J_{ij}, which average will hereafter be referred to as a ''sample-average'' following Refs. [6,11] and the number of realizations used will be denoted by N_s [12]. In that work, numerical integration was performed with the Euler scheme of time step $\Delta t = 2\pi \times 0.01$ for $N = 500,1000,2000$ and $N_s = 10$. For the larger values of N, J_c is near 6, and the exponent α depends on J [see Fig. 5(b) of Ref. [6]].

Recently, however, Stiller and Radons (SR) [13] have reported that their results are essentially different: they find exponential decay for $J<24.5$ and algebraic decay only for $J=24.5$, leaving the region $J>24.5$ unsettled because of the complex behavior of the order parameter therein. Their integration scheme is the Heun method with $\Delta t = 2\pi \times 10^{-3}$, which is expected to have better accuracy than the author's [6]. From this fact, they suggest that the slow relaxation found by the author is not correct, being a discretization effect due to the low order integration scheme. The main

It's complicated.

PHYSICAL REVIEW E VOLUME 58, NUMBER 2 AUGUST 1998

Dynamics of nonlinear oscillators with random interactions

J. C. Stiller and G. Radons*
Institut für Theoretische Physik, Universität Kiel, Olshausenstrasse 40, D-24118 Kiel, Germany
(Received 3 October 1997)

We develop a mean field theory for a system of coupled oscillators with random interactions with variable symmetry. Numerical simulations of the resulting one-dimensional dynamics are in accordance with simulations of the N-oscillator dynamics. We find a transition in dependence on interaction strength J and symmetry parameter η from a dynamically disordered phase to a phase with static disorder, where all oscillators are frozen in random positions. This transition between the ''paramagnetic'' phase and the spin glass phase appears to be of first order and is dynamically characterized by chaos (positive Lyapunov exponents) in the former case and regular motion (vanishing Lyapunov exponents) in the latter case. The Lyapunov spectrum shows an interesting symmetry for antisymmetric interaction ($\eta=-1$). [S1063-651X(98)14608-1]

PACS number(s): 05.45.+b, 05.70.Fh, 64.60.Ht, 64.60.Cn

I. INTRODUCTION

Oscillations and interacting oscillating systems are omnipresent in nature as well as in technical systems. Therefore, systems of coupled oscillators have received much interest in the last years. Synchronization and desynchronization were investigated for populations of fireflies [1,2], pacemaker cells of the heart, and pulsating lasers [3,39]. Oscillations in the nervous system [5], which control periodical processes as running, breathing, and chewing, received particular interest.

tion'' $m=(1/N)\Sigma_{j=1}^{N}\exp(i\phi_j)$ according to a power law in time. Our simulations with identical system size, smaller time discretization, and a numerical procedure of higher order do not confirm this result. We find a power law only for a critical interaction strength J_c; for $J>J_c$ and $J<J_c$, we do find systematic deviations from a power law. At J_c, however, the system shows a discontinuous transition from a dynamically disordered state to a spin glass state with frozen disorder, in contrast to the case of uniform and Van Hemmen type [20] interactions where the transition is con-

Daido (1992)

VOLUME 68, NUMBER 7 PHYSICAL REVIEW LETTERS 17 FEBRUARY 1992

Quasientrainment and Slow Relaxation in a Population of Oscillators with Random and Frustrated Interactions

Hiroaki Daido

Department of Physics, Faculty of Engineering, Kyushu Institute of Technology, Tobata, Kitakyushu 804, Japan

(Received 31 January 1991; revised manuscript received 22 October 1991)

It is numerically shown that there may be a new type of ordered state (in some sense glassy) in far-from-equilibrium systems which can be identified with a large population of coupled limit-cycle oscillators, provided couplings are not only random but also frustrated. It is characterized by quasientrainment and algebraic relaxation.

PACS numbers: 87.10.+e, 02.50.+s, 05.40.+j, 05.70.Fh

Large assemblies of coupled limit-cycle oscillators play an important role in many fields of science. Their most remarkable feature is that they exhibit macroscopic mutual entrainment for coupling strength greater than a certain threshold. The resulting coherent oscillations model a variety of rhythmic behaviors observed in diverse far-from-equilibrium systems, such as biological clocks, many physiological organisms, chemical reactors, and so on [1–3]. Quite a few investigations have been carried out analytically as well as numerically for a number of model systems in order to elucidate the nature of such a transition [2].

A common feature of the models used in those studies of coupled oscillators [4,7]. Suppose a pair of oscillators evolve as $\dot{\theta}_1 = \tilde{J}\sin 2\pi(\theta_2 - \theta_1 + \alpha_{21})$, $\dot{\theta}_2 = \tilde{J}\sin 2\pi(\theta_1 - \theta_2 + \alpha_{12})$, whose phase difference asymptotically becomes $\theta_1 - \theta_2 = \beta_{12} + \sigma_{12}$, where $\beta_{12} \equiv (\alpha_{21} - \alpha_{12})/2$ and $\sigma_{12} = 0$ or $\frac{1}{2}$ depending on the value of $\alpha_{12} + \alpha_{21}$. Then, imagine three oscillators, every pair of which has a similar coupling as above. It is easy to see that unless $\sum_{\text{pair}} (\beta_{ij} + \sigma_{ij}) = 0 (\text{mod} 1)$, the phase difference favored by the coupling cannot come true for *all* of the pairs, leading to a competition among interactions, or frustration. Extension is straightforward to the case of more than three oscillators.

Frustration may be a fairly common feature of real

Main dynamics: Daido's choices

$$\dot{\theta}_j = \omega_j + \sum_{k=1}^{N} J_{jk} \sin\left(\theta_k - \theta_j\right) \text{ for } j = 1, \ldots, N.$$

- Normally distributed natural frequencies.
- Symmetric coupling matrix ($J_{jk} = J_{kj}$), with entries distributed as Normal$(0, 2\pi J/\sqrt{N})$.

Daido's dynamics: $J < 8$

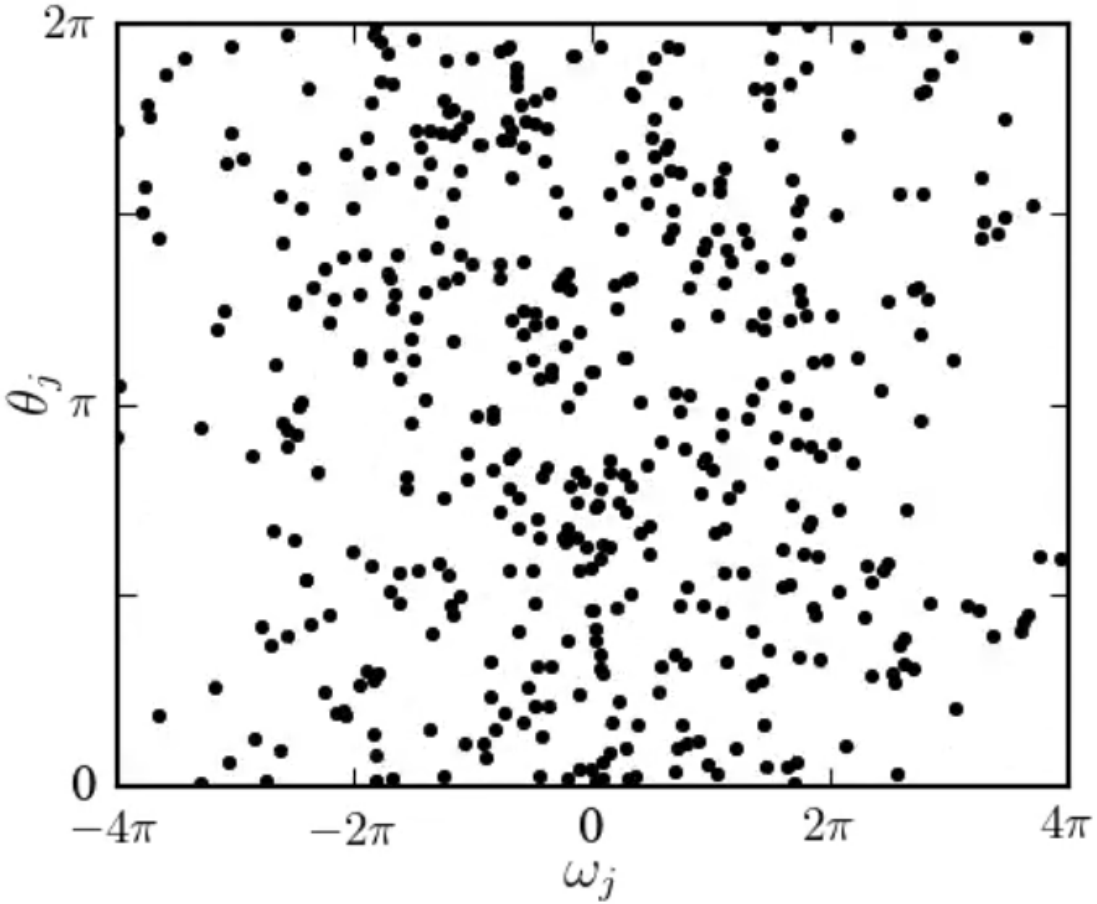

Figure: Phase Video Caption

Daido's dynamics: $J > 8$

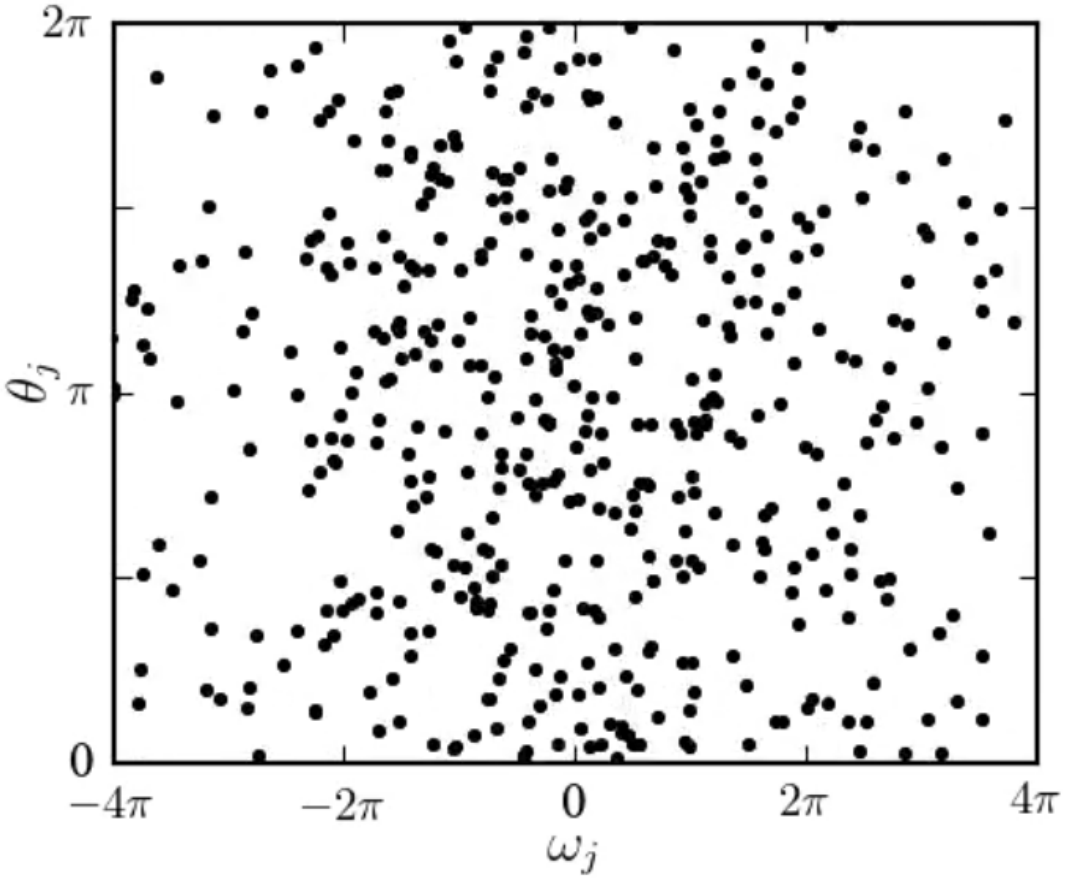

Figure: Phase Video Caption

Local Fields

We define the **local fields** to be

$$P_j = r_j e^{i\phi_j} := \sum_{k=1}^{N} J_{jk} e^{i\theta_k},$$

for $j = 1, \ldots, N$. Equation (1) then becomes

$$\dot{\theta}_j = \omega_j + r_j \sin\left(\phi_j - \theta_j\right).$$

Daido (1992): Local field trajectories

Expand

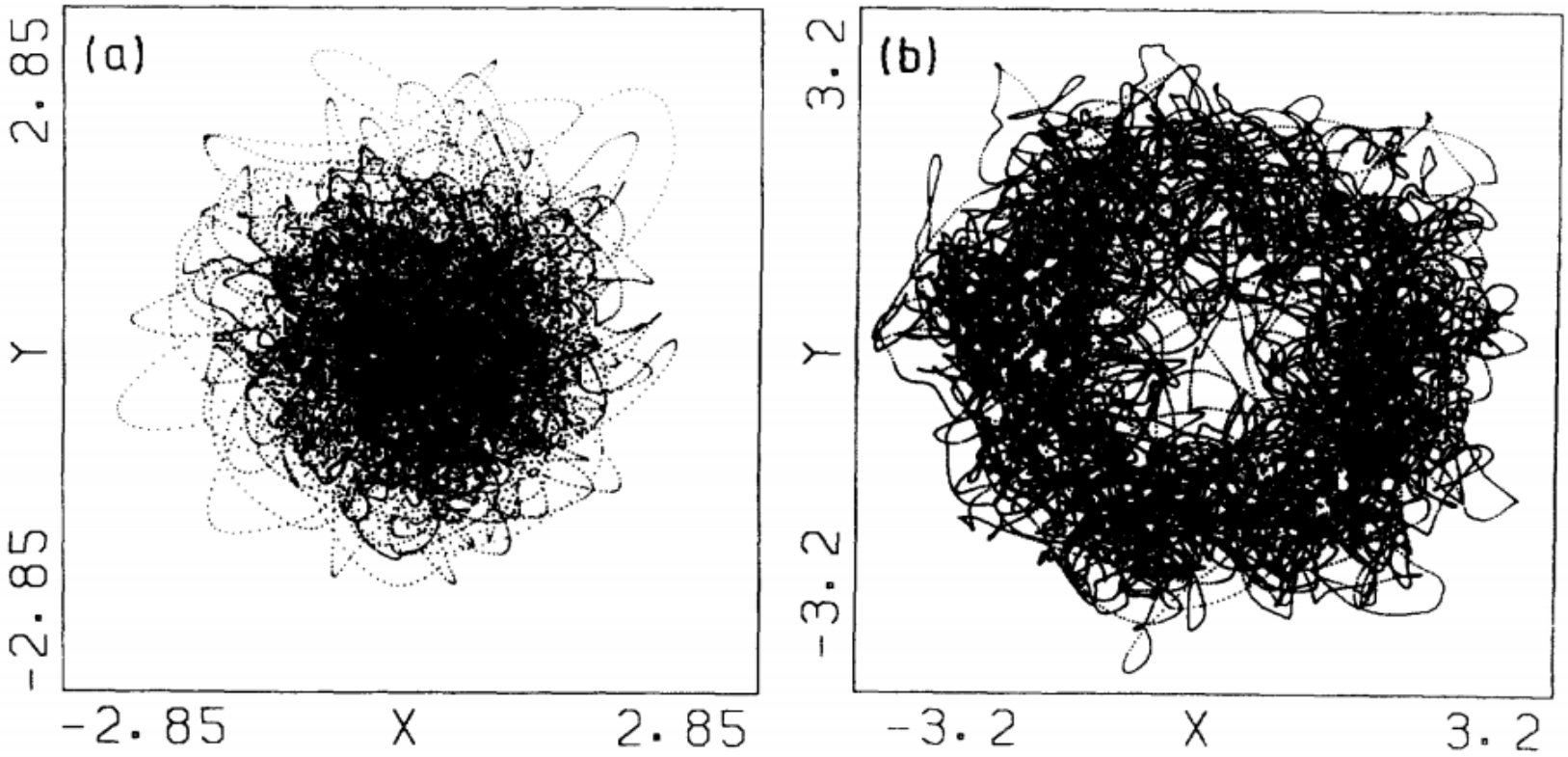

FIG. 1. Phase portraits of a local field ($N=500$): (a) $J=4$ (20000 points); (b) $J=14$ (50000 points).

Daido (1992): a volcano transition

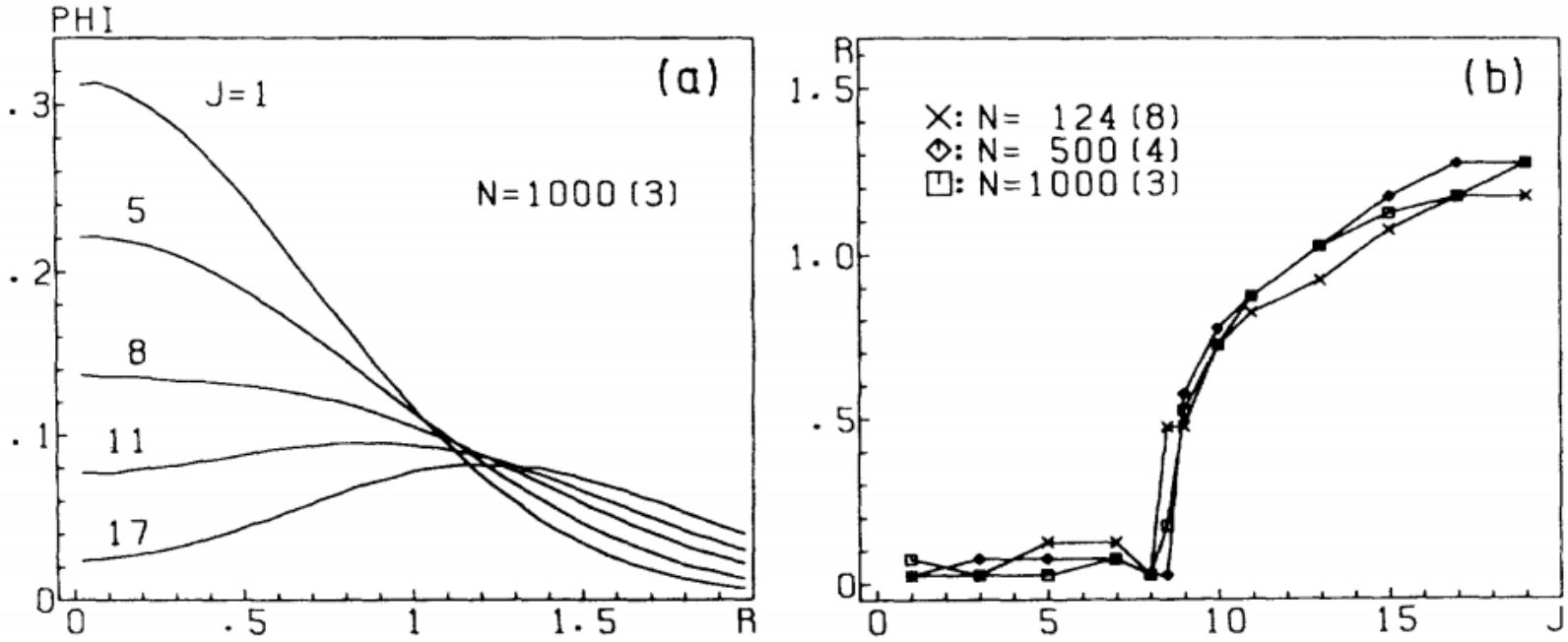

FIG. 2. Behavior of the distribution of a local field averaged over all j: (a) $\mathrm{PHI}(R) \equiv P(x,y)$ vs $R = (x^2+y^2)^{1/2}$, where P is averaged over three samples of J_{ij} as is expressed by (3) in the figure (this convention will be used hereafter); (b) the peak point of $\mathrm{PHI}(R)$ vs J.

Daido (1992): a volcano transition

Claim

There is some critical coupling scale J_c that corresponds to the onset of a volcano transition. Moreover, this corresponds to a transition into a glassy state.

Main dynamics: our choices

Main dynamics: our choices

Instead of normally distributed natural frequencies, we use the Cauchy distribution

$$g(\omega) = \frac{1}{\pi(1+\omega^2)}.$$

Main dynamics: our choices

Instead of normally distributed couplings, we make

$$J_{jk} = \frac{J}{N} \sum_{m=1}^{K} (-1)^m u_m^{(j)} u_m^{(k)}, \tag{2}$$

where each u is iid, with equal probability of being ± 1.

The coupling matrix: special features

$$J_{jk} = \frac{J}{N} \sum_{m=1}^{K} (-1)^m u_m^{(j)} u_m^{(k)}.$$

The coupling matrix: special features

$$J_{jk} = \frac{J}{N} \sum_{m=1}^{K} (-1)^m u_m^{(j)} u_m^{(k)}.$$

- J controls the spread.

The coupling matrix: special features

$$J_{jk} = \frac{J}{N} \sum_{m=1}^{K} (-1)^m u_m^{(j)} u_m^{(k)}.$$

- J controls the spread.
- K controls the rank, since it decides the number of outer products making J_{jk} (Even Integer).

The coupling matrix: interpretation

$$J_{jk} = \frac{J}{N} \sum_{m=1}^{K} (-1)^m u_m^{(j)} u_m^{(k)}.$$

- Each oscillator j has a vector $\left(u_1^{(j)}, \ldots, u_K^{(j)}\right)$, and the coupling between oscillators j and k depends on the number of places their vectors agree.

The coupling matrix: extra features Expand

$$J_{jk} = \frac{J}{N} \sum_{m=1}^{K} (-1)^m u_m^{(j)} u_m^{(k)}.$$

- If $K = N$ and $N \to \infty$, then the off-diagonal entries go to Normal$(0, J/\sqrt{N})$. **(Has relevant limit)**

Local Fields (reminder)

We define the local fields to be

$$P_j = r_j e^{i\phi_j} := \sum_{k=1}^{N} J_{jk} e^{i\theta_k},$$

for $j = 1, \ldots, N$. Equation (1) then becomes

$$\dot{\theta}_j = \omega_j + r_j \sin\left(\phi_j - \theta_j\right).$$

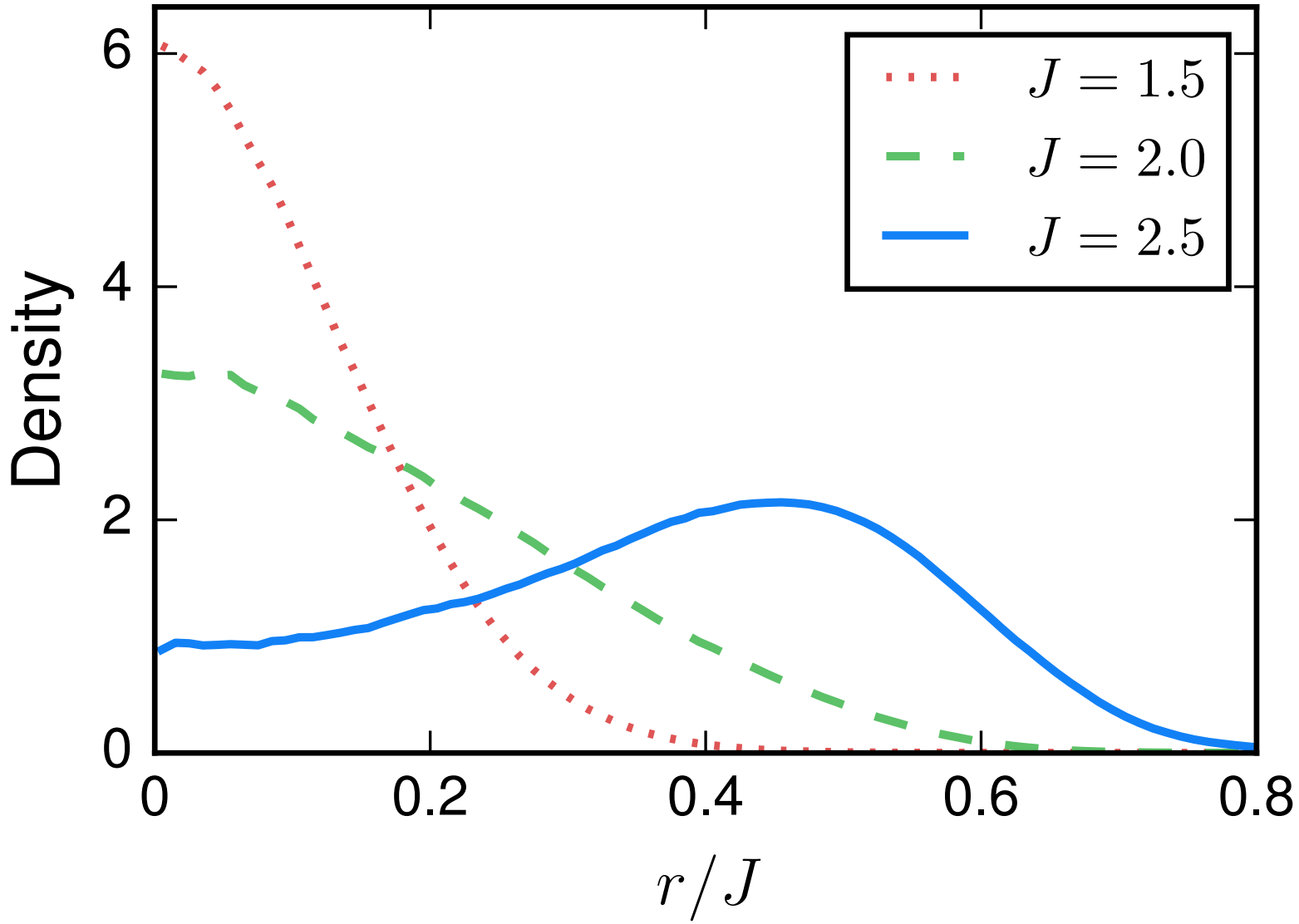
Density
6
4
2
0
0
0.2
0.4
0.6
0.8
r/J
$J = 1.5$
$J = 2.0$
$J = 2.5$

Infinite N

Infinite N

$f(\theta, \omega, u, t) =$ density of oscillators with natural frequency ω, interaction vector u, and phase θ at time t.

$\nu(\theta, \omega, u, t) =$ flow of ditto.

Infinite N: interaction matrix

Much the same as before:

$$J(u, u') := J \sum_{m=1}^{K} (-1)^m u_m u'_m.$$

The u's are random K-vectors with entries being ± 1 with equal probability, so

$$\rho(u') = 2^{-K} \sum_{v} \delta(u' - v),$$

where the sum runs over all the equally likely $v \in \{\pm 1\}^K$.

Infinite N: putting it together Expand

So

$$\dot{\theta}_j = \omega_j + \sum_{k=1}^{N} J_{jk} \sin(\theta_k - \theta_j)$$

becomes

$$\nu(\theta, \omega, u, t) = \omega + \langle J(u, u') \sin(\theta' - \theta) \rangle, \tag{3}$$

$\langle \cdot \rangle$ denotes integration using the time-dependent measure $f(\theta', \omega', u', t) d\theta' g(\omega') d\omega' \rho(u') du'$.

Infinite N: local fields again

Also,

$$P_j = r_j e^{i\phi_j} := \sum_{k=1}^{N} J_{jk} e^{i\theta_k},$$

becomes

$$P(u,t) = \langle J(u,u') e^{i\theta'} \rangle.$$

The Ott-Antonsen Ansatz

$$f(\theta, \omega, u, t) = \frac{1}{2\pi}\left[1 + \sum_{n=1}^{\infty} \alpha(\omega, u, t)^n e^{in\theta} + \text{c.c.}\right]$$

Following the conventions and defining $a(u,t) := \alpha(-i,u,t)$, we find

$$\dot{a}(u,t) = -a(u,t) + \frac{P^*(u,t) - a(u,t)^2 P(u,t)}{2}. \qquad (4)$$

The ansatz also simplifies the local fields into

$$P(u,t) = \frac{J}{2^K} \sum_{u'} \sum_{m=1}^{K} (-1)^m u_m u'_m a^*(u',t).$$

Time to Ott

By replacing P with its sum, we get a closed set of 2^K ordinary differential equations for $a(u, t)$, one for each possible choice of u.

Stability?

- We have a 2^K dimensional ODE.

Stability?

- We have a 2^K dimensional ODE.
- $a(u,t) = 0 \implies f(\theta, \omega, u, t) = 1/(2\pi)$, which is incoherence.

Stability?

- We have a 2^K dimensional ODE.
- $a(u,t) = 0 \implies f(\theta, \omega, u, t) = 1/(2\pi)$, which is incoherence.
- J_c, the critical coupling, corresponds to the incoherent state no longer being stable.

Stability?

- We have a 2^K dimensional ODE.
- $a(u,t) = 0 \implies f(\theta, \omega, u, t) = 1/(2\pi)$, which is incoherence.
- J_c, the critical coupling, corresponds to the incoherent state no longer being stable.
- **To calculate J_c, we just need to linearize this ODE and find the first zero eigenvalue.**

The Jacobian is

$$-I + \frac{J}{2^{K+1}} A. \tag{5}$$

Here I is the $2^K \times 2^K$ identity matrix and

$$A_{u,v} = \sum_{m=1}^{K} (-1)^m u_m v_m$$

where the entries of A have been conveniently indexed by binary strings $u, v \in \{\pm 1\}^K$.

Since the Jacobian is

$$-I + \frac{J}{2^{K+1}} A,$$

the Jacobian has exactly three distinct eigenvalues:

1. $-1 + J/2$ with multiplicity $K/2$
2. $-1 - J/2$ with multiplicity $K/2$
3. -1 with multiplicity $2^K - K$

Main Result:

Theorem

$$J_c = 2. \tag{6}$$

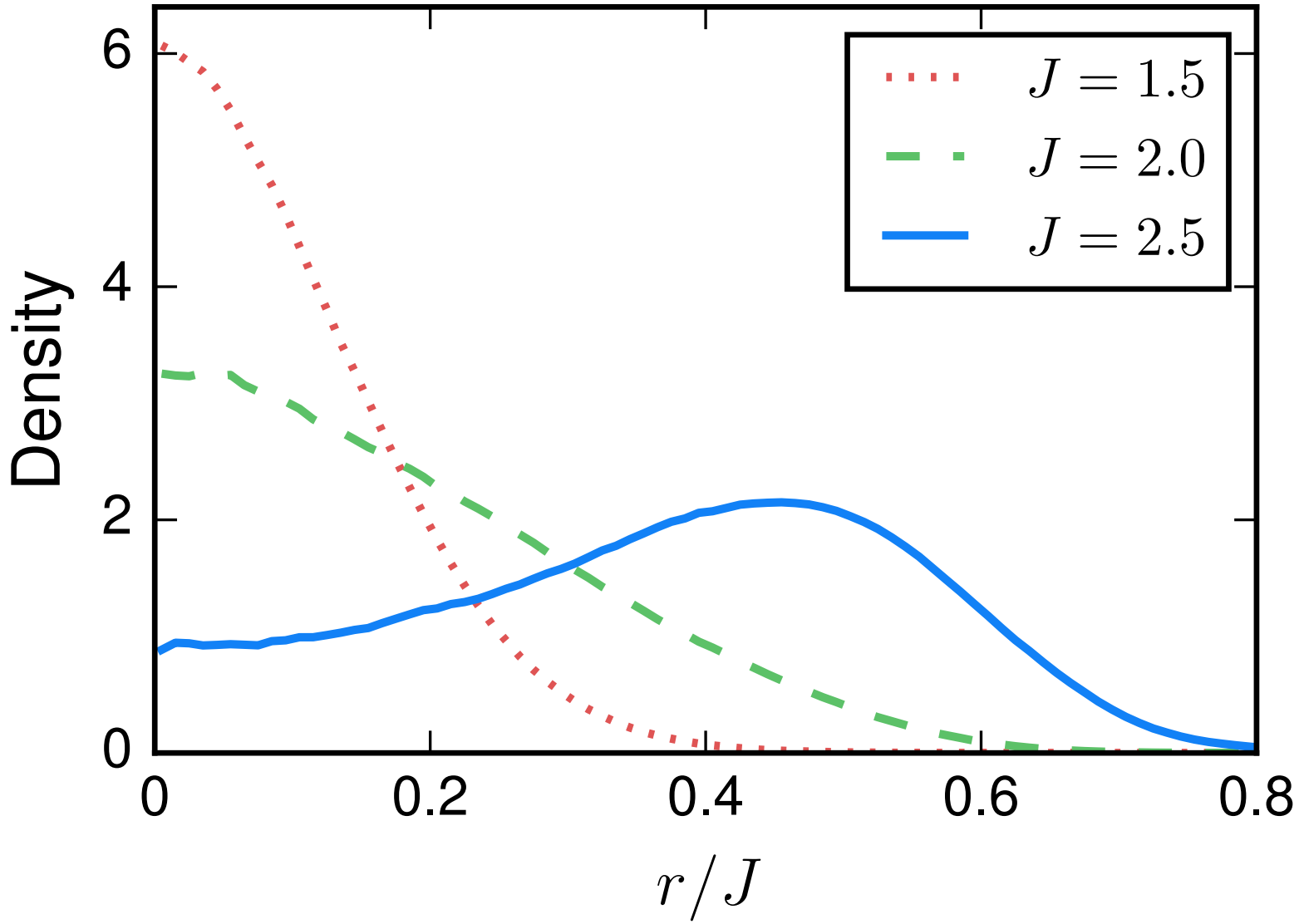
Density
6
4
2
0
0
0.2
0.4
0.6
0.8
r/J
$J = 1.5$
$J = 2.0$
$J = 2.5$

Numerical checks?

Numerical checks: it's complicated. Expand

Convergence to $J_c = 2$ Expand

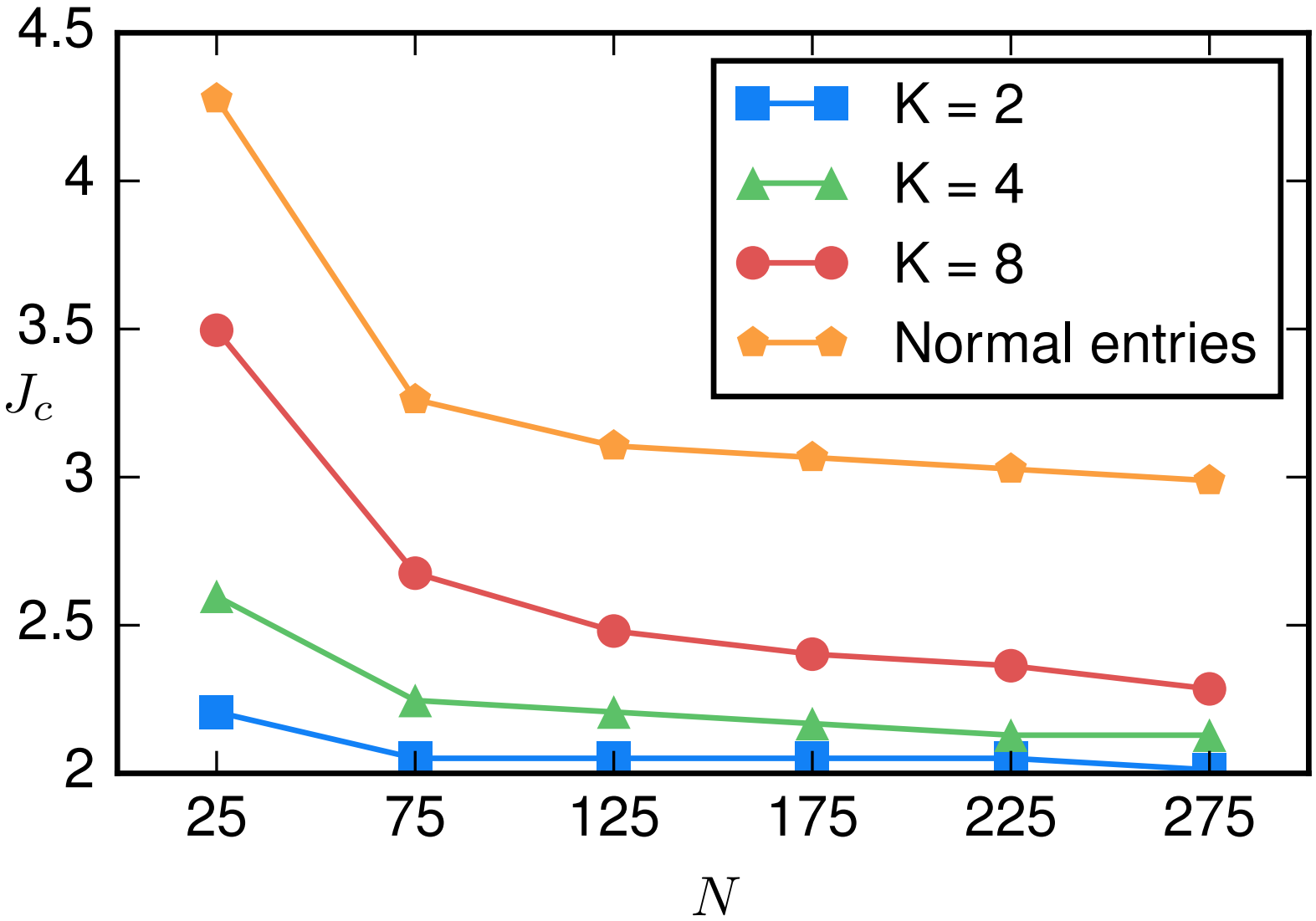

Are we a glass yet?

Are we a glass yet?

A proposed signature feature of oscillator glasses is nonexponential relaxation of the order parameter

$$Z(t) := \sum_{k=1}^{N} e^{i\theta_k(t)}.$$

No. Expand

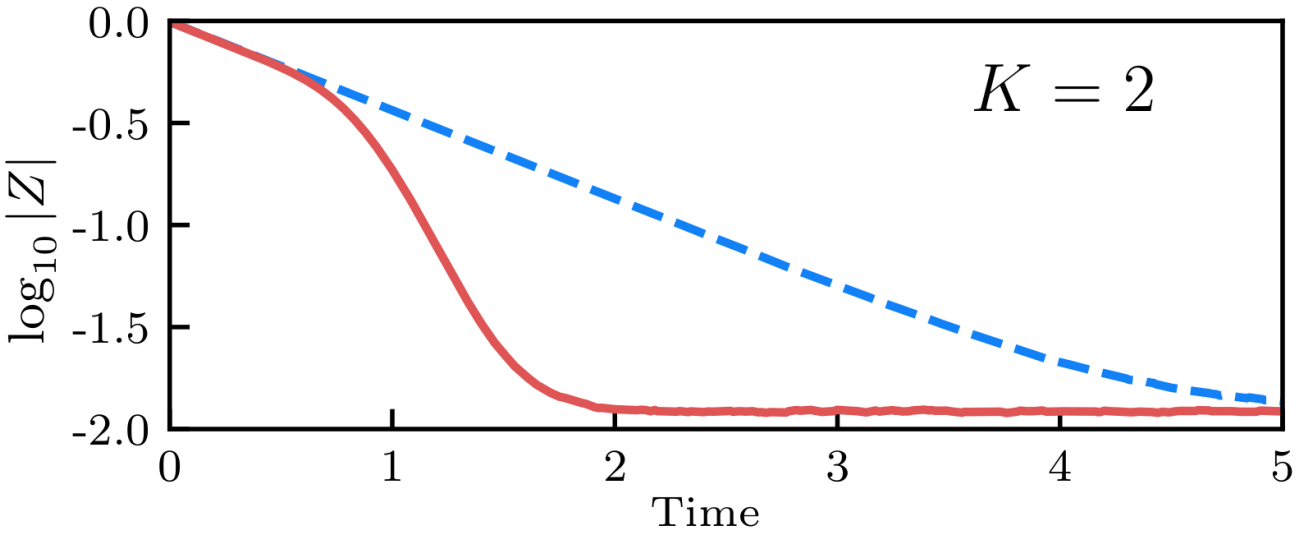

Figure: Dashed blue line has $J = 0$. Solid red has $J = 10$. $N = 5000$ for both.

Is a glass possible?

- Our continuum limit gives us 2^K ODEs.
- Therefore, it is only consistent when $\boldsymbol{N \gg 2^K}$
- What if that doesn't happen?

Algebraic decay? Expand

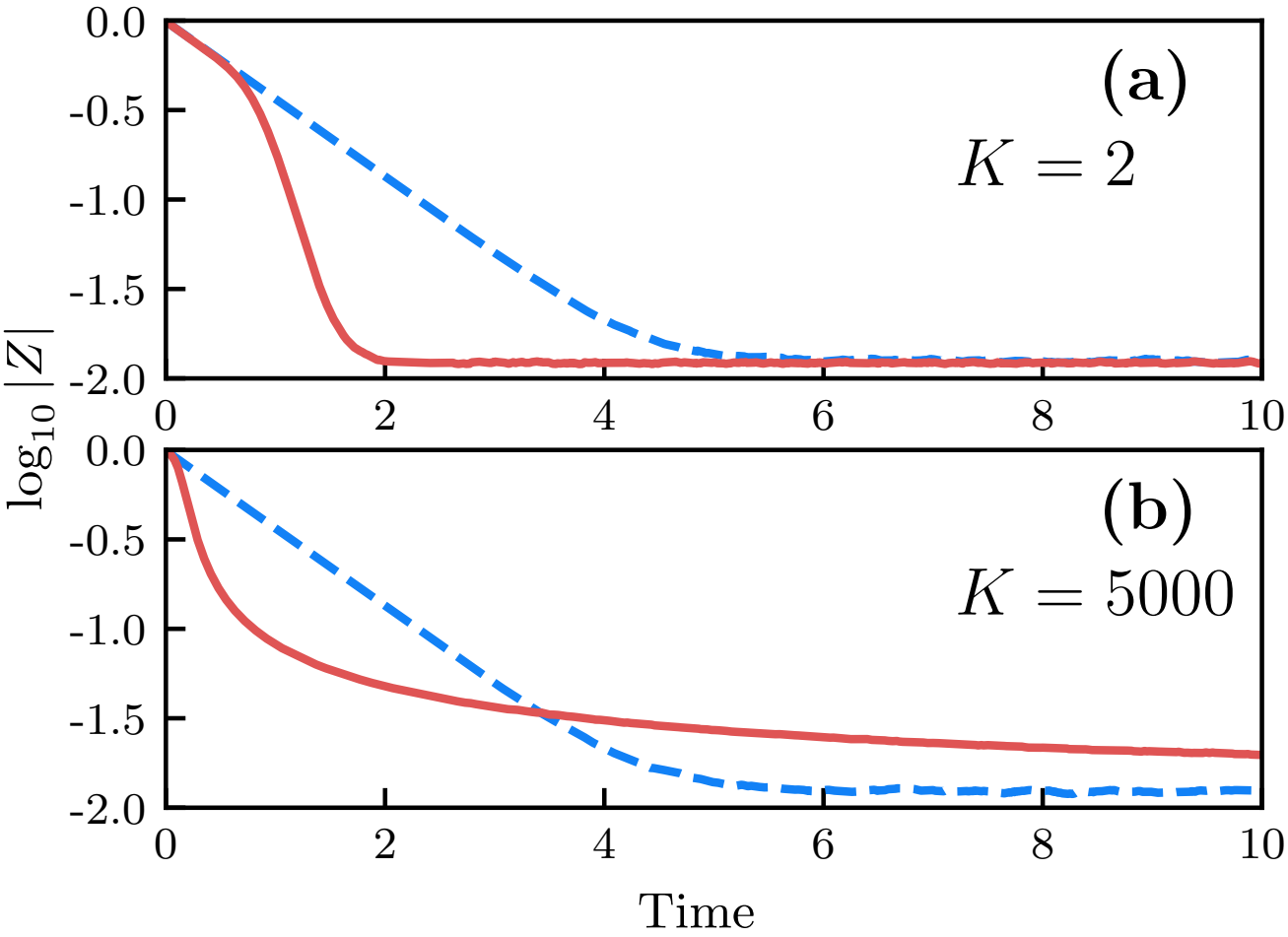

Figure: Dashed blue line has $J = 0$. Solid red has $J = 10$. $N = 5000$ for both.

Algebraic decay? Expand

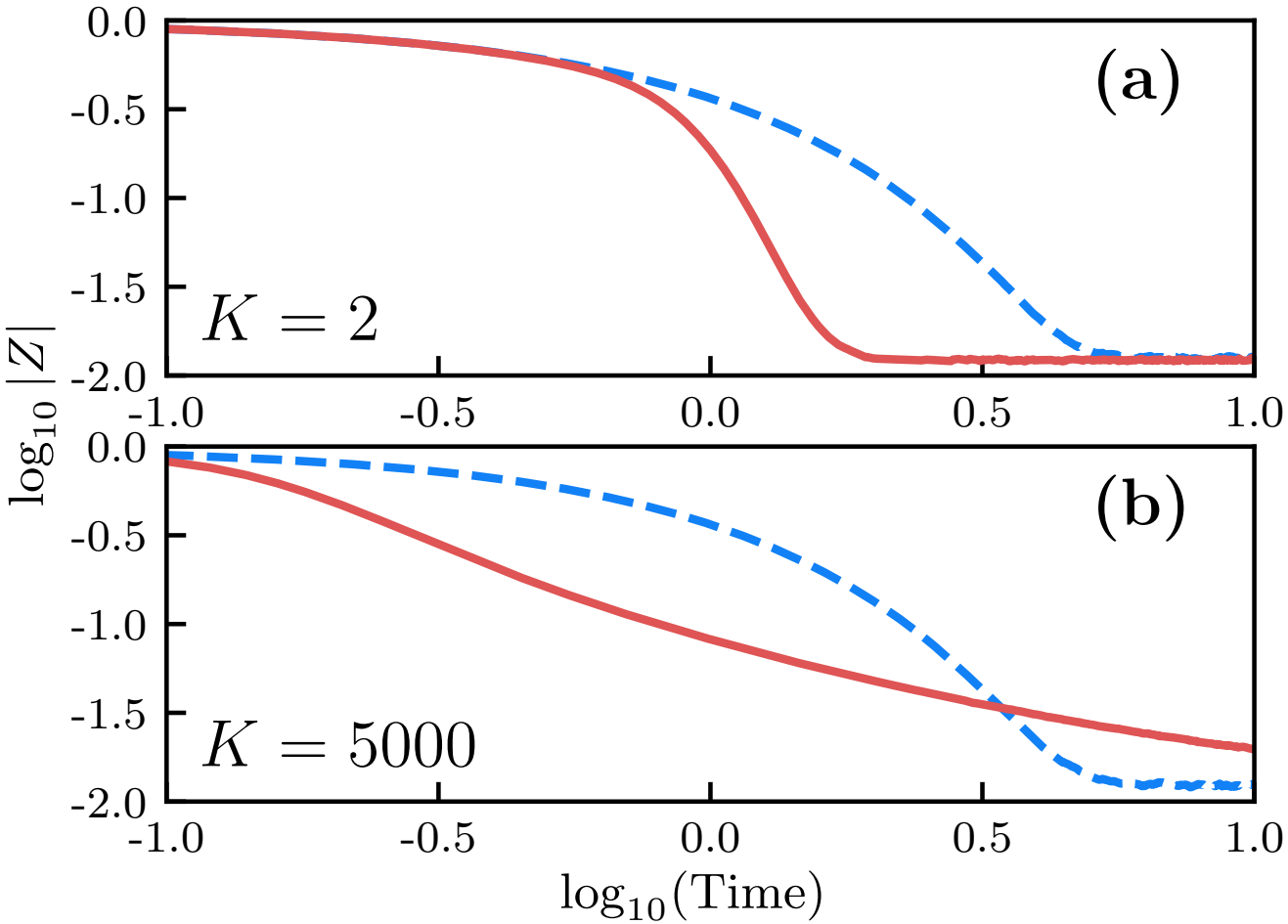

Figure: Dashed blue line has $J = 0$. Solid red has $J = 10$. $N = 5000$ for both.

Final Summary

- $J_c = 2$, regardless of the rank of the coupling matrix.
- The volcano transition can occur in absence of a glass transition.
- There is still the possibility of a glass transition in the high K limit of this model.

Future directions

Future directions

Checking the large K limit for glassy behavior.

Future directions

Applying results to associative memory models:

$$J_{jk} = \frac{J}{N} \sum_{m=1}^{K} (1 - \delta_{jk}) e^{\mu_m^{(j)}} e^{\mu_m^{(k)}}$$

with each $\mu_m^{(j)}$ being uniform on 0-2π.

Future directions

Semi-field parameters are set by

$$F_m = \sum_{k=1}^{N} u_m^{(k)} e^{i\theta_k}.$$

These have many fun properties, including their relationship to local fields:

$$P_j = \frac{J}{N} \sum_{m=1}^{K} (-1)^m u_m^{(j)} F_m.$$

They also make for good videos: Example Caption

Selected References


B. Ottino-Löffler, S. H. Strogatz, Phys. Rev. Lett. 120, 264102 (2018).


H. Daido, Prog. Theor. Phys. 77, 622 (1987).


H. Daido, Phys. Rev. Lett. 68, 1073 (1992).


J. Stiller and G. Radons, Phys. Rev. E 58, 1789 (1998).


H. Daido, Phys. Rev. E 61, 2145 (2000).


J. Stiller and G. Radons, Phys. Rev. E 61, 2148 (2000).


D. Sherrington and S. Kirkpatrick, Phys. Rev. Lett. 35, 1792 (1975).


D. Iatsenko, P. V. McClintock, and A. Stefanovska, Nature Communications 5 (2014).

This research was supported by a Sloan Fellowship to Bertrand Ottino-Löffler, in the Center for Applied Mathematics in Cornell, as well as by NSF grants DMS-1513179 and CCF-1522054.

Questions? (Full slides available at ottinoloffler.com)

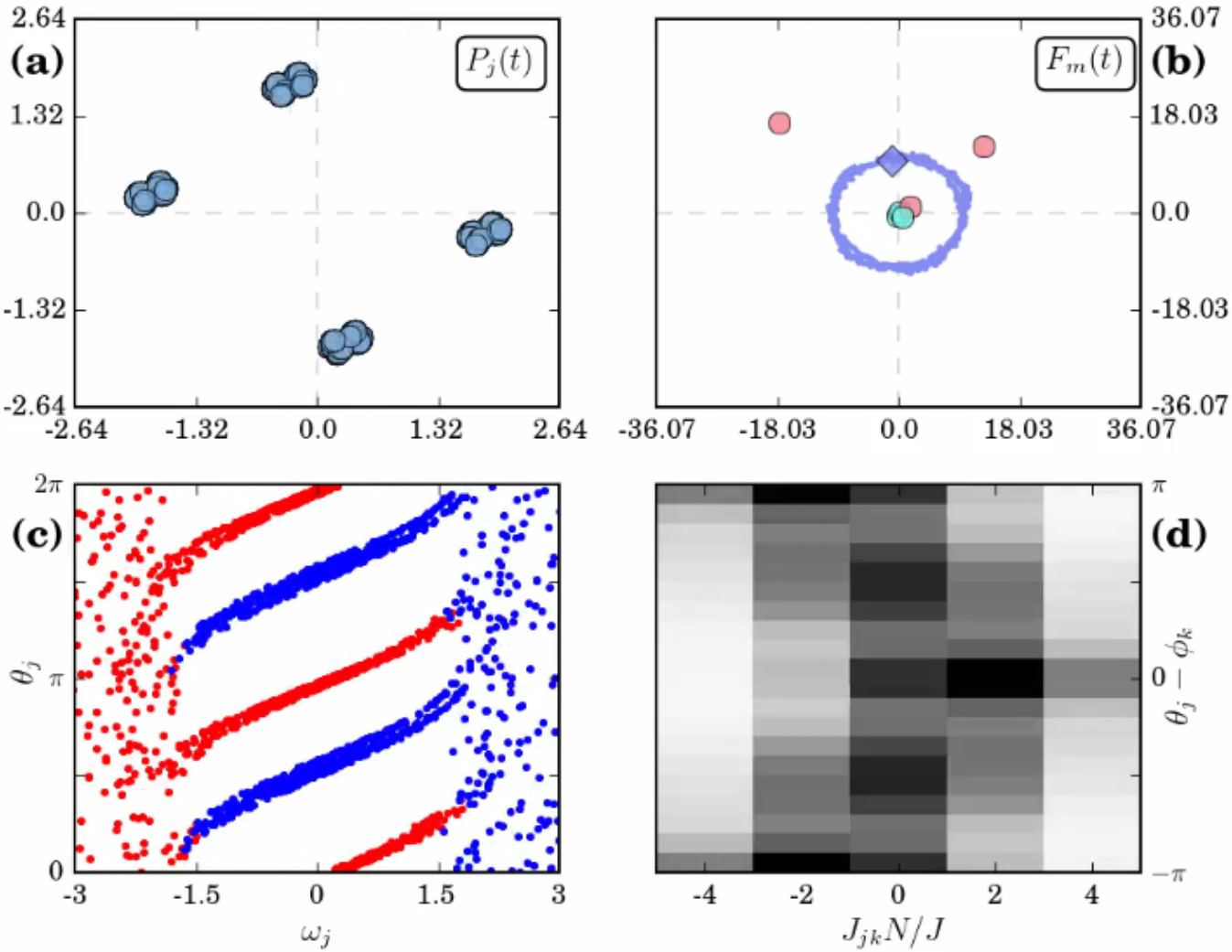

Figure: Summary Video Full Caption

Daido's dynamics: $J < 8$ Return

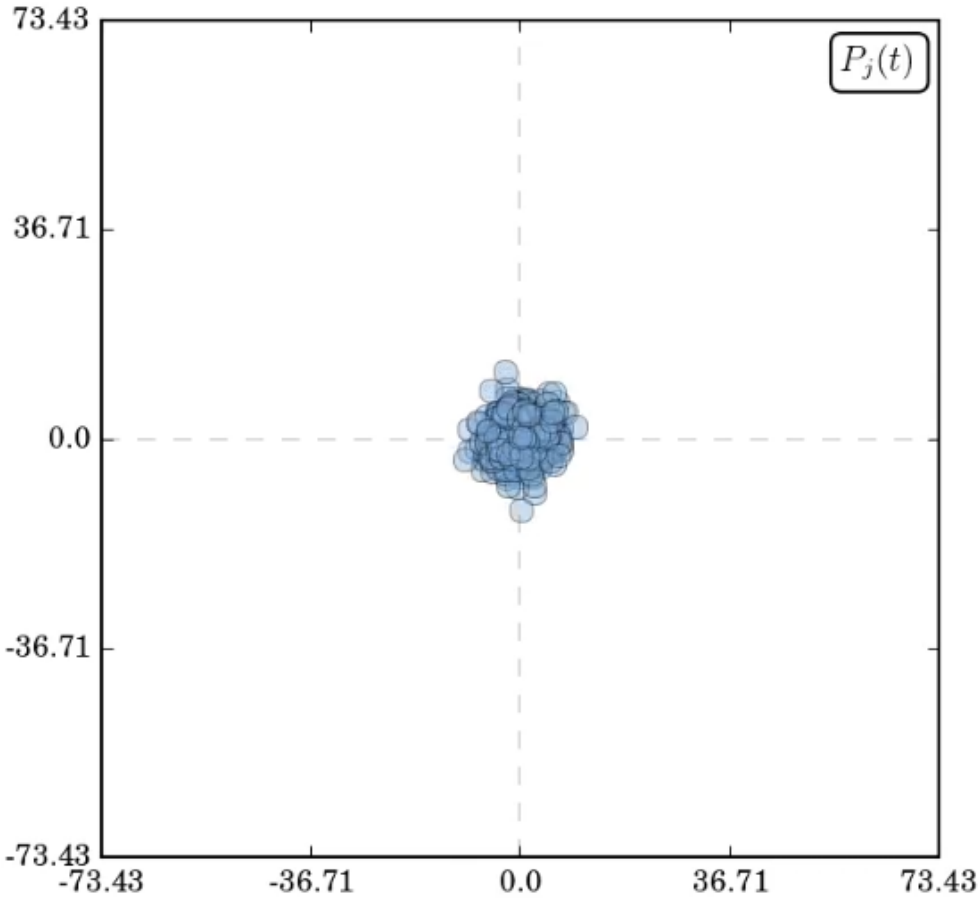

Figure: Field Video Caption

Daido's dynamics: $J > 8$ Return

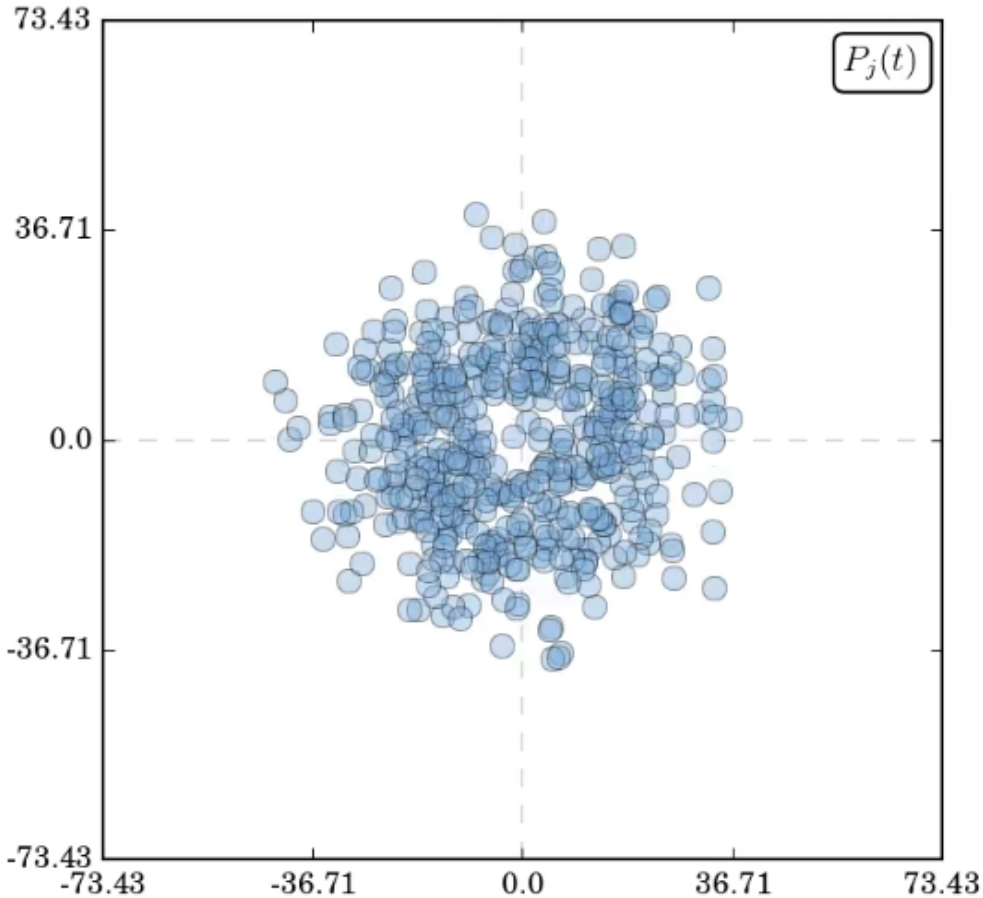

Figure: Field Video Caption

The coupling matrix: extra features Return

$$J_{jk} = \frac{J}{N} \sum_{m=1}^{K} (-1)^m u_m^{(j)} u_m^{(k)}.$$

- Outer products make it **symmetric.**

The coupling matrix: extra features Return

$$J_{jk} = \frac{J}{N} \sum_{m=1}^{K} (-1)^m u_m^{(j)} u_m^{(k)}.$$

- Outer products make it **symmetric.**
- $(-1)^m$ ensures the diagonal is 0 **(No spurious information)**

The coupling matrix: extra features Return

$$J_{jk} = \frac{J}{N} \sum_{m=1}^{K} (-1)^m u_m^{(j)} u_m^{(k)}.$$

- Outer products make it **symmetric.**
- $(-1)^m$ ensures the diagonal is 0 **(No spurious information)**
- If $K = N$ and $N \to \infty$, then the off-diagonal entries go to Normal$(0, J/\sqrt{N})$. **(Has relevant limit)**

The coupling matrix: extra features

Return

$$J_{jk} = \frac{J}{N} \sum_{m=1}^{K} (-1)^m u_m^{(j)} u_m^{(k)}.$$

- Outer products make it **symmetric.**
- $(-1)^m$ ensures the diagonal is 0 **(No spurious information)**
- If $K = N$ and $N \to \infty$, then the off-diagonal entries go to Normal$(0, J/\sqrt{N})$. **(Has relevant limit)**
- Entries of J_{jk} are **independent.** (Are they?)

Yes, they are (I) Return

The only chance of non-trivial dependence is between entries of the same row or column of the coupling matrix, that is, between J_{jk} and J_{jl}.

Yes, they are (II) Return

Take some $x, y \in \{0, 1, \ldots, K\}$, then

$$\mathcal{P} := P\left(\frac{N}{J} J_{\boldsymbol{j}k} = 2x - K \text{ and } \frac{N}{J} J_{\boldsymbol{j}l} = 2y - K\right)$$

$$= P\left(\sum_{m=1}^{K} (-1)^m u_m^{(j)} u_m^{(k)} = 2x - K \text{ and } \sum_{m=1}^{K} (-1)^m u_m^{(j)} u_m^{(l)} = 2y - K\right)$$

Let $a_m := (-1)^m u_m^{(j)}$, $b_m := u_m^{(k)}$, $c_m := u_m^{(l)}$.

Yes, they are (III) Return

Let $a_m := (-1)^m u_m^{(j)}$, $b_m := u_m^{(k)}$, $c_m := u_m^{(l)}$.
Each can be thought of as a fair K-long coinflip sequence of $+1$'s and -1's.

$$\mathcal{P} = P\left(\sum_{m=1}^{K} a_m b_m = 2x - K \text{ and } \sum_{m=1}^{K} a_m c_m = 2y - K\right)$$

$$= P(\text{ coinflip sequence } a \text{ agrees with } b \ x \text{ times and with } c \ y \text{ times })$$

$$= \binom{K}{x}\binom{K}{y} 2^{-2K}$$

$$= P\left(\frac{N}{J} J_{jk} = 2x - K\right) P\left(\frac{N}{J} J_{jl} = 2y - K\right) \checkmark$$

Yes, they are (IV) Return

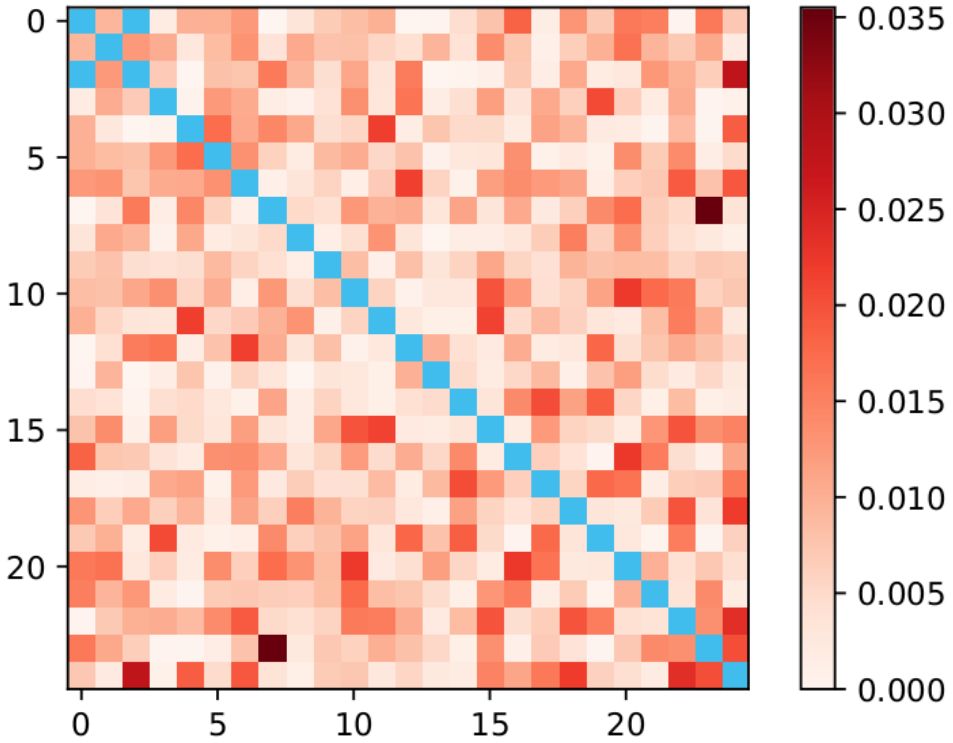

Figure: Measuring absolute correlation between $J_{1,2}$ and $J_{j,k}$ across a coupling matrix of size $N = 25$ and $K = 4$, averaged across 10^5 realizations. Blue entries (the diagonal, (1,2), and (2,1)) have trivial correlations and are ignored.

Phase distributions for $J = 1$ Return

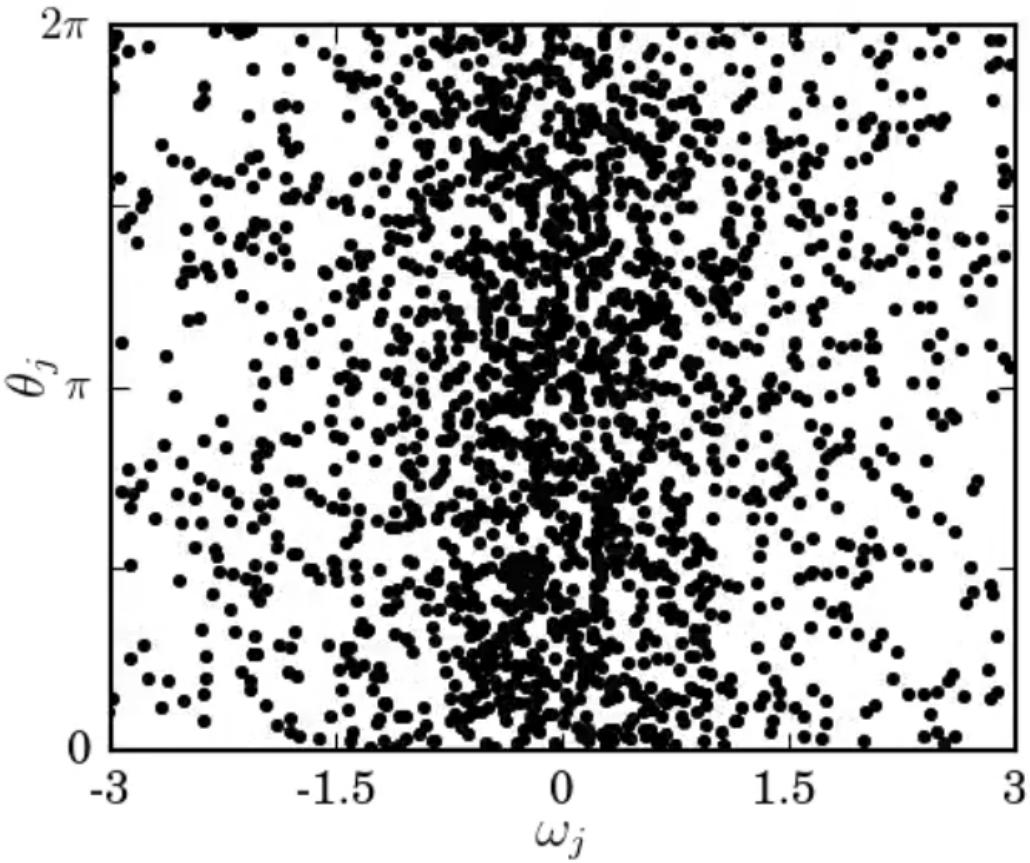

Figure: Phase Video Full Caption

Phase distributions for $J = 3$ Return

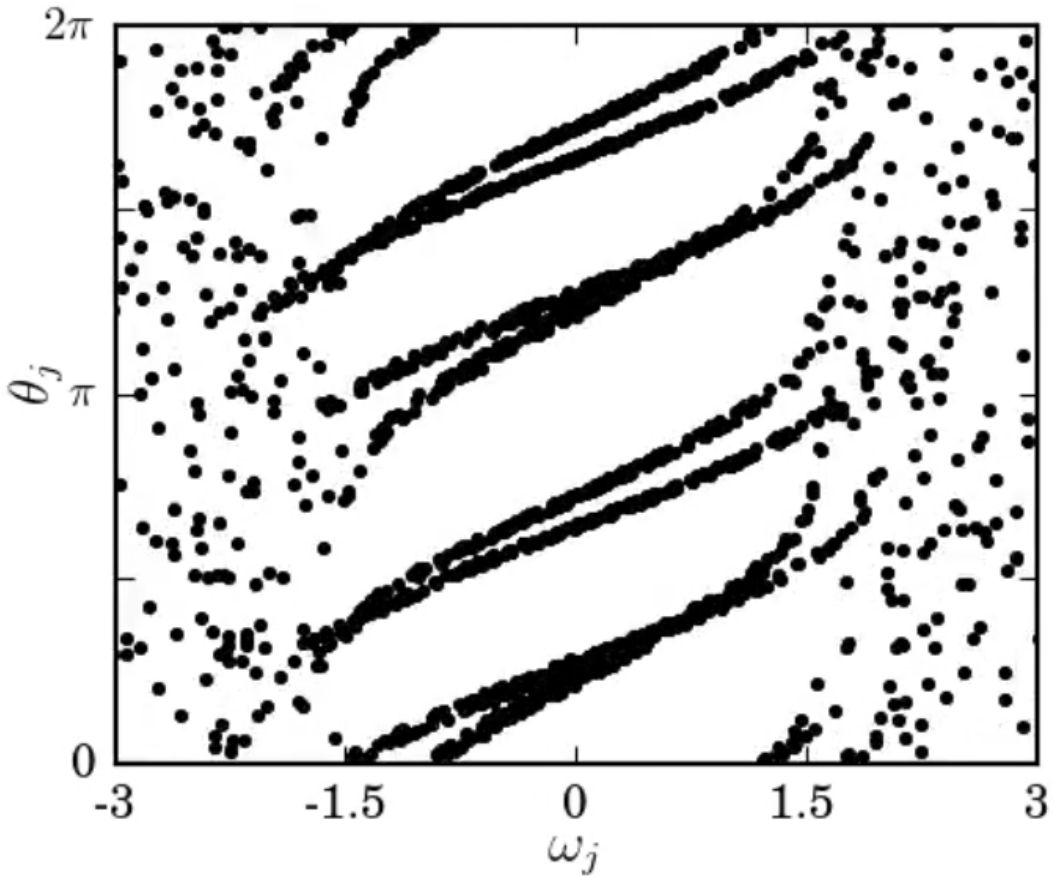

Figure: Phase Video Full Caption

Local Fields for $J = 1$ Return

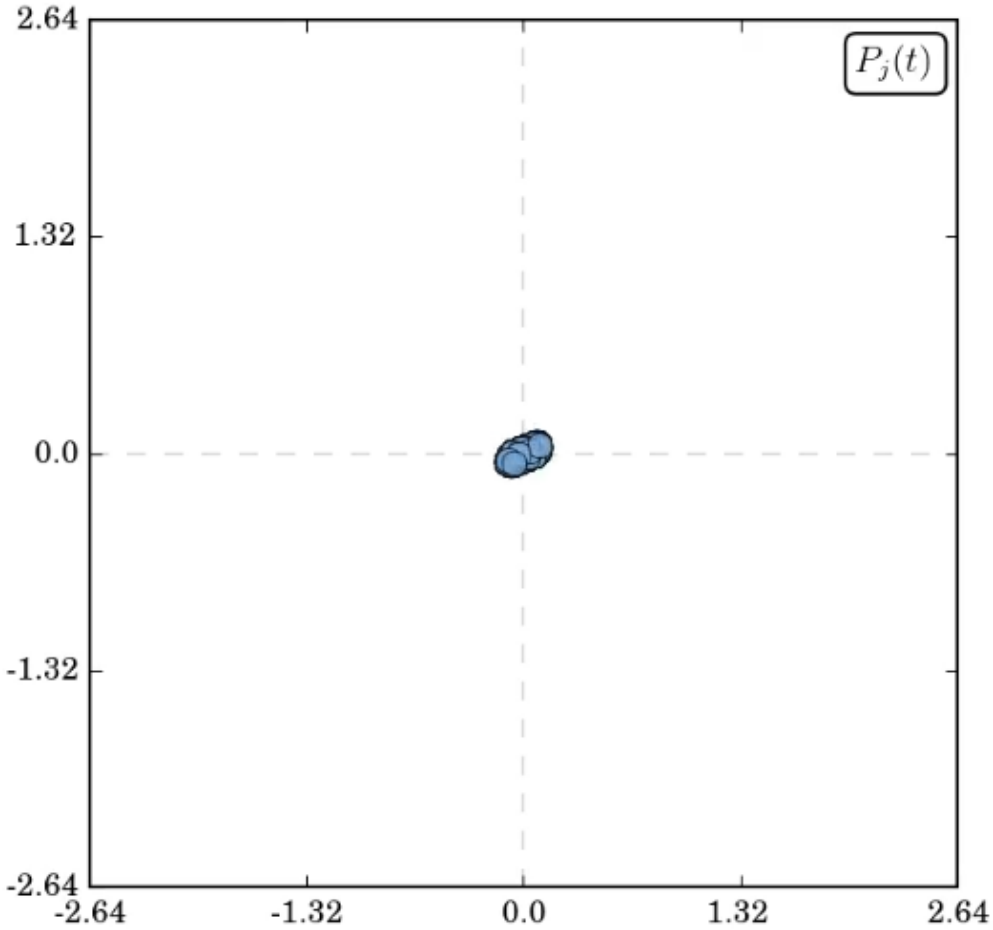

Figure: Field Video Full Caption

Local Fields for $J = 3$ Return

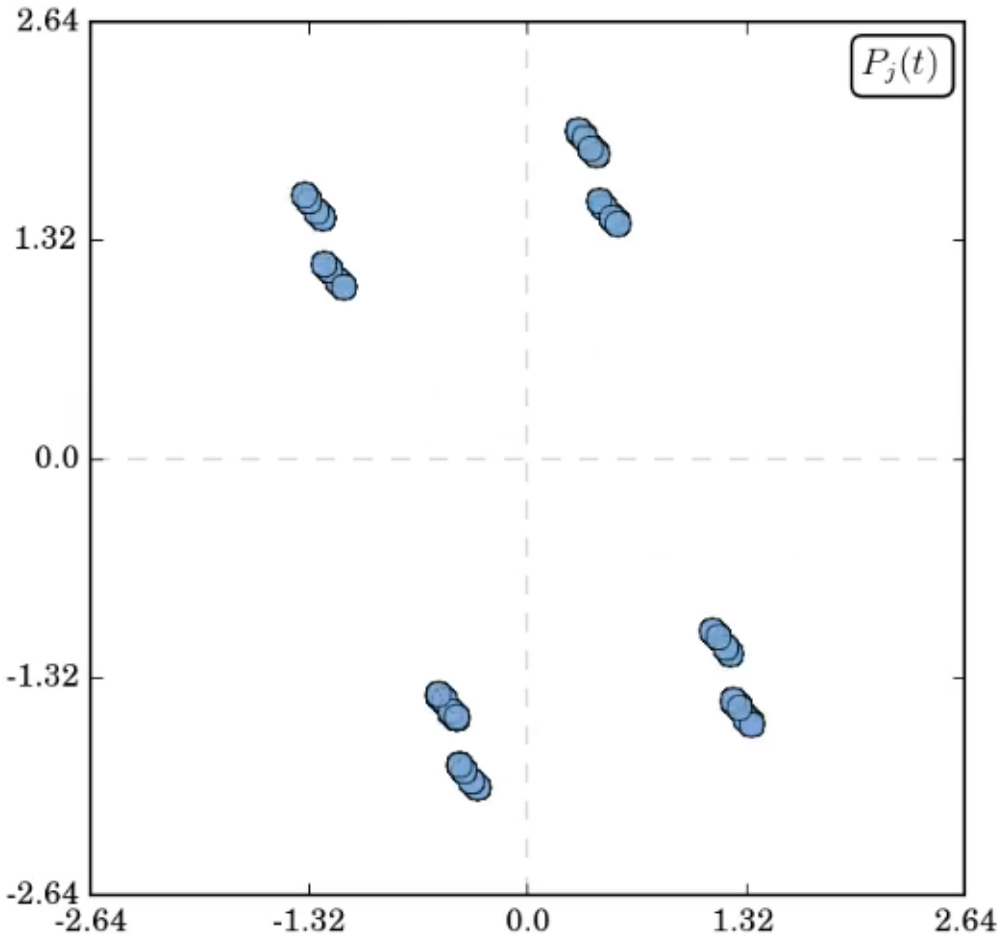

Figure: Field Video Full Caption

Continuum limit explanation (I) Return

How does

$$\dot{\theta}_j = \omega_j + \sum_{k=1}^{N} J_{jk} \sin\left(\theta_k - \theta_j\right)$$

become

$$\nu(\theta, \omega, u, t) = \omega + \langle J(u, u') \sin(\theta' - \theta) \rangle ? \tag{7}$$

Continuum limit explanation (II) Return

Since

$$J(u,u') := J\sum_{m=1}^{K}(-1)^m u_m u'_m.$$

we get

$$\dot{\theta}_j = \omega_j + \sum_{k=1}^{N}\frac{1}{N}J\left(u^{(j)},u^{(k)}\right)\sin\left(\theta_k-\theta_j\right).$$

Continuum limit explanation (III) Return

Consider adding a hypothetical oscillator with phase θ, natural frequency ω, and interaction vector u. Then its instantaneous frequency would be given by

$$\nu(\theta, \omega, u, t) = \omega + \sum_{k=1}^{N} \frac{1}{N} J\left(u, u^{(k)}\right) \sin\left(\theta_k - \theta\right).$$

Continuum limit explanation (IV) Return

Sums are just integrals, so

$$\nu(\theta, \omega, u, t) = \omega + \int J\left(u, u'\right) \sin\left(\theta_k - \theta\right) \mu d\theta' d\omega' du',$$

where we have the normalized measure

$$\mu := \frac{1}{N} \sum_{k=1}^{N} \delta\left(\theta' - \theta_k\right) \delta\left(\omega' - \omega_k\right) \delta\left(u' - u^{(k)}\right).$$

Continuum limit explanation (V) Return

Let's slightly overload our terminology by introducing

$$\hat{\theta}(k,\omega,u,t) = \begin{cases} \theta_k(t) \text{ if } \omega = \omega_k \text{ and } u = u^{(k)}, \\ 0 \text{ else.} \end{cases}$$

Continuum limit explanation (VI) Return

Naturally,

$$\lim_{N\to\infty} \frac{1}{N} \sum_{k=1}^{N} \delta\left(\omega - \omega_k\right) = g(\omega)$$

$$\lim_{N\to\infty} \frac{1}{N} \sum_{k=1}^{N} \delta\left(u - u^{(k)}\right) = \rho(u).$$

But now, we define a new measure

$$f(\theta, \omega, u, t) := \lim_{N\to\infty} \frac{1}{N} \sum_{k=1}^{N} \delta\left(\theta - \hat{\theta}(k, \omega, u, t)\right).$$

Continuum limit explanation (VII) Return

Because u and ω are independent, we find that

$$\begin{aligned}\mu =& \frac{1}{N}\sum_{k=1}^{N}\delta\left(\theta'-\theta_k\right)\delta\left(\omega'-\omega_k\right)\delta\left(u'-u_k\right)\\ =& \frac{1}{N}\sum_{k=1}^{N}\delta\left(\theta'-\hat{\theta}(k,\omega,u,t)\right)\delta\left(\omega'-\omega_k\right)\delta\left(u'-u_k\right)\\ & \xrightarrow{N\to\infty} f(\theta,\omega,u,t)g(\omega)\rho(u)\end{aligned}$$

Continuum limit explanation (VIII) Return

So in the large N limit, we find that

$$\nu(\theta, \omega, u, t) = \omega + \langle J(u, u') \sin(\theta' - \theta) \rangle,$$

where $\langle \cdot \rangle$ denotes integration using the time-dependent measure $f(\theta', \omega', u', t) d\theta' g(\omega') d\omega' \rho(u') du'$. ✓

Ott trick explanation (I) Return

How

$$f(\theta,\omega,u,t)=\frac{1}{2\pi}\left[1+\sum_{n=1}^{\infty}\alpha(\omega,u,t)^n e^{in\theta}+\text{c.c.}\right]$$

becomes

$$\dot{a}(u,t)=-a(u,t)+\frac{P^*(u,t)-a(u,t)^2P(u,t)}{2}.$$

Ott trick explanation (II) Return

Because the total number of oscillators doesn't change, a continuity equation must be obeyed. In particular,

$$-f_t = (f\nu)_\theta.$$

Ott trick explanation (III) Return

LHS first.

$$
\begin{aligned}
-f_t =& \partial_t \frac{-1}{2\pi}\left[1+\sum_{n=1}^{\infty}\alpha(\omega,u,t)^n e^{in\theta}+\text{c.c.}\right] \\
=& \frac{-1}{2\pi}\sum_{n=1}^{\infty} n\dot{\alpha}\alpha^{n-1}e^{in\theta}+n\dot{\alpha}^*\alpha^{*n-1}e^{-in\theta}
\end{aligned}
$$

Ott trick explanation (IV) Return

Now RHS . . .
After some manipulation, this:

$$\nu(\theta, \omega, u, t) = \omega + \langle J(u, u') \sin(\theta' - \theta) \rangle,$$

becomes this:

$$\nu(\theta, \omega, u, t) = \omega + \frac{1}{2i} \left[e^{-i\theta} P(u, t) - e^{i\theta} P^*(u, t) \right].$$

Ott trick explanation (V) Return

RHS takes more work than LHS ...

$$f\nu = \frac{1}{2\pi}\left[1 + \sum_{n=1}^{\infty} \alpha^n e^{in\theta} + \alpha^* n e^{-in\theta}\right]\left[\omega + \frac{1}{2i}\left(e^{-i\theta}P - e^{i\theta}P^*\right)\right].$$

Ott trick explanation (VI) Return

But eventually ...

$$
\begin{aligned}
f\nu = & \frac{1}{4\pi i}\left[2\omega i + \alpha P - \alpha^* P^*\right] \\
& + \frac{1}{4\pi i}\sum_{n=1}^{\infty}\left(2\omega i\alpha^n + \alpha^{n+1}P - \alpha^{n-1}P^*\right)e^{in\theta} \\
& + \frac{1}{4\pi i}\sum_{n=1}^{\infty}\left(2\omega i\alpha^{*n} - \alpha^{*n+1}P^* + \alpha^{*n-1}P\right)e^{-in\theta}.
\end{aligned}
$$

Ott trick explanation (VII) Return

And so ...

$$(f\nu)_\theta = \frac{1}{4\pi i}\sum_{n=1}^{\infty}(in)\left(2\omega i\alpha^n + \alpha^{n+1}P - \alpha^{n-1}P^*\right)e^{in\theta}$$
$$+ \frac{1}{4\pi i}\sum_{n=1}^{\infty}(-in)\left(2\omega i\alpha^{*n} - \alpha^{*n+1}P^* + \alpha^{*n-1}P\right)e^{-in\theta}.$$

Ott trick explanation (VIII) Return

By setting $f_t + (f\nu)_\theta = 0$ and setting Fourier coefficients to be equal, then

$$\dot{\alpha} = -\omega\alpha i + \frac{P^* - \alpha^2 P}{2}$$

Ott trick explanation (IX) Return

The calculation of $P(u,t)$ reveals it only depends on $\alpha(-i,u,t)$, so setting $\omega = -i$ and $a(u,t) := \alpha(-i,u,t)$, we finally get

$$\dot{a}(u,t) = -a(u,t) + \frac{P^*(u,t) - a(u,t)^2 P(u,t)}{2}.\checkmark$$

Another trick explanation (I) Return

How

$$P(u,t) = \langle J(u,u')e^{i\theta'} \rangle$$

becomes

$$P(u,t) = \frac{J}{2^K} \sum_{u'} \sum_{m=1}^{K} (-1)^m u_m u'_m a^*(u',t).$$

Another trick explanation (II) Return

Sub in the ansatz to get

$$P(u,t) = \int J(u,u')e^{i\theta'} f(\theta',\omega',u',t)g(\omega')\rho(u')d\theta' d\omega' du'$$

$$= \int \frac{J(u,u')}{2\pi}\left[e^{i\theta'} + \sum_{n=1}^{\infty} \alpha^n e^{i(n+1)\theta} + \alpha^* n e^{-i(n-1)\theta}\right]$$

$$g(\omega')\rho(u')d\theta' d\omega' du'.$$

Another trick explanation (III) Return

Take the θ' integral first to get rid of almost everything

$$P(u,t) = \int \frac{J(u,u')}{2\pi}(2\pi\alpha^*)g(\omega')\rho(u')d\omega' du'$$
$$= \int J(u,u')\alpha^* g(\omega')\rho(u')d\omega' du'.$$

Another trick explanation (IV) Return

Next, we want to take the ω' integral. Since we are using a Cauchy distribution, then

$$g(\omega) = \frac{1}{\pi(a+\omega^2)} = \frac{i/(2\pi)}{\omega+i} + \frac{-i/(2\pi)}{\omega-i}.$$

So if α has the right smoothness and decay, then the integrand has exactly two poles at $\pm i$.

Another trick explanation (V) Return

So by taking the appropriate contour integral, we get

$$\begin{aligned} P(u,t) &= \int J(u,u') \left(\int \alpha^*(\omega', u', t) g(\omega') d\omega' \right) \rho(u') du' \\ &= \int J(u,u') \left(-2\pi i \frac{i}{2\pi} \alpha^*(-i, u', t) \right) \rho(u') du' \\ &= \int J(u,u') a(u',t) \rho(u') du', \end{aligned}$$

where $a(u,t) := \alpha(-i,u,t)$.

Another trick explanation (VI) Return

From here, just plug in for J, recalling that $\rho(u') = 2^{-K} \sum_v \delta(u' - v)$

$$P(u,t) = \int J(u,u')a(u',t)\rho(u')du'$$

$$= \frac{J}{2^K} \sum_{u'} \sum_{m=1}^{K} (-1)^m u_m u'_m a^*(u',t).\checkmark$$

Why that Jacobian? (I) Return

How

$$\dot{a}(u,t) = -a(u,t) + \frac{P^*(u,t) - a(u,t)^2 P(u,t)}{2}.$$

becomes

$$-I + \frac{J}{2^{K+1}} A.$$

Why that Jacobian? (II) Return

- We want to linearize around $a(u,t) = 0$ for all u.
- P and P^* are just $O(a)$.
- Therefore, we can drop the $a^2 P$ term near 0.

Why that Jacobian? (III) Return

Therefore, near the incoherent state,

$$\dot{a}(u,t) \approx -a(u,t) + \frac{1}{2}P^*(u,t) + O(a^2)$$

$$\approx -a(u,t) + \frac{J}{2^{K+1}} \sum_{u'} \sum_{m=1}^{K} (-1)^m u_m u'_m a(u',t)$$

Why that Jacobian? (IV) Return

So the entries of the Jacobian are given by

$$\partial_{a(u)}\dot{a}(u) = -1 + \frac{J}{2^{K+1}}\sum_{m=1}^{K}(-1)^m u_m u_m$$

$$= -1 + \frac{J}{2^{K+1}}\sum_{m=1}^{K}(-1)^m = -1$$

on the diagonal, and

$$\partial_{a(v)}\dot{a}(u) = \frac{J}{2^{K+1}}\sum_{m=1}^{K}(-1)^m u_m v_m$$

of the off-diagonal.

Why that Jacobian? (V) Return

The most convenient way to index the entries of the Jacobian is by using the vectors $u, v \in \{+1, -1\}^K$, AKA the set of all K-long binary strings. So entry u, v of the Jacobian is

$$-\delta_{u,v} + \frac{J}{2^{K+1}} \sum_{m=1}^{K} (-1)^m u_m v_m$$

Why that Jacobian? (VI) Return

Therefore, the Jacobian is

$$-I + \frac{J}{2^{K+1}} A,$$

where I is the $2^K \times 2^K$ identity matrix and

$$A_{u,v} = \sum_{m=1}^{K} (-1)^m u_m v_m . \checkmark$$

For each integer $1 \leq n \leq K$ and each binary string $v \in \{\pm 1\}^K$, define a vector $\zeta^{(n)} \in \mathbb{R}^{2^K}$ whose vth entry is

$$\zeta_v^{(n)} = v_n.$$

Features of $\zeta^{(n)}$? Return

- The set of all K distinct $\zeta^{(n)}$ are orthogonal. (Are they?)
- By using the evenness of K, then $A\zeta^{(n)} = (-1)^n 2^K \zeta^{(n)}$. (Really?)

Other eigens? Return

Given any η perpendicular to all the $\zeta^{(n)}$, one finds $A\eta = 0$.

Therefore, A has exactly three distinct eigenvalues:

1. $+2^K$ with multiplicity $K/2$
2. -2^K with multiplicity $K/2$
3. 0 with multiplicity $2^K - K$

Yes, they are orthogonal (I) Return

Why is

$$\zeta_v^{(n)} = v_n,$$

orthogonal for all n?

Yes, they are orthogonal (II) Return

Let $n \neq m$,

$$\zeta^{(n)}\zeta^{(m)} = \sum_{v} v_n v_m.$$

Yes, they are orthogonal (III) Return

Let $n \neq m$, then

$$\begin{aligned}
\zeta^{(n)}\zeta^{(m)} &= \sum_{v} v_n v_m \\
&= |\{\#\text{ times } m \text{ and } n \text{ agree}\}| \\
&\quad - |\{\#\text{ times } m \text{ and } n \text{ disagree}\}| \\
&= 2^{K-2}(1+1) - 2^{K-2}(1+1) \\
&= 0. \checkmark
\end{aligned}$$

Yes, they are eigenvectors (I) Return

Why does

$$A_{uv} = \sum_{m=1}^{K} (-1)^m u_m v_m$$

have

$$\zeta_v^{(n)} = v_n,$$

as an eigenvector?

Yes, they are eigenvectors (II) Return

Let's do this directly, and let's fix some $n \in \{1, 2, \ldots, K\}$ and $u \in \{+1, -1\}^K$. So

$$\begin{aligned}
\left(A\zeta^{(n)}\right)_u &= \sum_v A_{uv}\zeta_v^{(n)} = \sum_v \left(\sum_{m=1}^{K}(-1)^m u_m v_m\right) v_n \\
&= \sum_{m=1}^{K}\sum_v (-1)^m u_m v_m v_n \\
&= \sum_v (-1)^n u_n v_n v_n + \sum_{m\neq n}\sum_v (-1)^m u_m v_m v_n \\
&= \text{Term 1} + \text{Term 2}
\end{aligned}$$

Yes, they are eigenvectors (III) Return

First term!

$$\begin{aligned}\text{Term } 1 &= \sum_{v}(-1)^n u_n v_n v_n \\ &= (-1)^n u_n \sum_{v} v_n^2 \\ &= (-1)^n 2^K u_n\end{aligned}$$

Yes, they are eigenvectors (IV) Return

The second term therefore becomes

$$\begin{aligned}\text{Term } 2 &= \sum_{m\neq n}\sum_{v\in\{\pm 1\}^K} (-1)^m u_m v_m v_n \\ &= \sum_{m\neq n}\sum_{v'\in\{\pm 1\}^{K-1}} u'_m v'_m,\end{aligned}$$

where the u' and v' are n-deleted versions of $(-1)^m u_m$ and $v_m v_n$ specifically.

Yes, they are eigenvectors (V) Return

Second term becomes a matter of just counting the number of places two vectors u' and v' of length $K-1$ disagree, across all possible v'. So combinatorically,

$$\text{Term } 2 = 2\sum_{w=0}^{K-1}(K-1-2w)\binom{K-1}{w}.$$

Yes, they are eigenvectors (VI) Return

But . . .

$$\begin{aligned}\text{Term } 2 =& 2\sum_{w=0}^{K-1}(K-1-2w)\binom{K-1}{w}\\ =& 0.\end{aligned}$$

This is an odd function times an even function, so the total sum goes to zero. (Really?)

Yes, they are eigenvectors (VII) Return

Putting them back together ...

$$\begin{aligned}\left(A\zeta^{(n)}\right)_u &= \text{Term 1} + \text{Term 2} \\ &= (-1)^n 2^K u_n + 0 \\ &= (-1)^n 2^K \zeta_u^{(n)}, \forall u.\end{aligned}$$

Therefore, for all n, we have

$$A\zeta^{(n)} = (-1)^n 2^K \zeta^{(n)}. \checkmark$$

Showing the nullspace (I) Return

Why does

$$\eta \perp \zeta^{(n)} \text{ for all } n$$

imply

$$A\eta = 0?$$

Showing the nullspace (II) Return

Since

$$\eta \perp \zeta^{(n)} \text{ for all } n,$$

then for any $n = 1, 2, \ldots, K$, we have

$$\eta\zeta^{(n)} = 0.$$

Showing the nullspace (III) Return

Therefore,

$$
\begin{aligned}
(A\eta)_u &= \sum_v A_{uv}\eta_u = \sum_v \sum_{m=1}^{K} (-1)^m u_m v_m \eta_u \\
&= \sum_{m=1}^{K} (-1)^m u_m \sum_v v_m \eta_u = \sum_{m=1}^{K} (-1)^m u_m \left(\eta \zeta^{(n)}\right) \\
&= \sum_{m=1}^{K} (-1)^m u_m 0 = 0.
\end{aligned}
$$

So $A\eta = 0$, so it forms a nullspace. ✓.

Numerical checks: Daido's method Return

Measure the location of the peak:

1. If the peak is at zero, the we are below the transition
2. Otherwise, we are above it.

Daido problematic Return

Measure the location of the peak:

- Radial density noisiest at origin.
- Need to collect and add many pdfs, but ignore most of the data in diagnosis.
- Binning of pdfs will be arbitrary.

Numeircal checks: our method Return

Fit the radial distribution of the data to symmetric normals

$$h(r) = \frac{1}{\sqrt{2\pi\sigma^2}} \exp\left(\frac{-(r-\mu)^2}{2\sigma^2}\right) + \frac{1}{\sqrt{2\pi\sigma^2}} \exp\left(\frac{-(r+\mu)^2}{2\sigma^2}\right)$$

for $r \geq 0$.

The functional form of $h(r)$ allows us to identify its convexity at the origin easily.

- $\gamma := \mu^2/\sigma^2 < 1$ implies **concave down**.
- $\gamma > 1$ implies **concave up**.

Measuring γ? Return

We are going to use method of moments on the 2D local field data, with M_n being the n'th moment.

Measuring γ? Expand Return

$$M_{+1}M_{-1} = \frac{\pi}{2}\frac{1+\gamma}{[e^{-\gamma/2} + \sqrt{\pi\gamma/2}\mathrm{Erf}(\sqrt{\gamma/2})]^2}.$$

- The left hand side comes from simulation data. Expand
- The right hand side is monotone in γ. Expand
- Therefore, $h(r)$ is concave down at the origin (and therefore $J < J_c$) if and only if $M_{+1}M_{-1} \gtrsim 1.4694$.

Concavity (I) Return

When is the sum of two normals centered at $\pm\mu$ concave up at the origin?

Concavity (II) Return

When is

$$h(r) = \frac{2}{\sqrt{2\pi\sigma^2}} \exp\left(\frac{-\mu^2 - r^2}{2\sigma^2}\right) \cosh\left(\frac{\mu r}{\sigma^2}\right),$$

concave up at the origin?

Concavity (III) Return

Letting $\gamma := \mu^2/\sigma^2$ and $\beta := \mu/\sigma^2$,

$$h(r) = \frac{2\beta}{\sqrt{2\pi\gamma}} \exp\left(\frac{-\gamma}{2}\right) \exp\left(\frac{-r^2\beta^2}{2\gamma}\right) \cosh(r\beta).$$

Concavity (IV) Return

$$\partial_r^2 h(r) = \beta^3 \gamma^{-2} \exp\left(\frac{-\gamma}{2} - \frac{\beta^2 r^2}{2\gamma}\right) \sqrt{\frac{2}{\pi\gamma}}$$
$$\times \cosh(\beta r)\left[-\gamma + \gamma^2 + \beta^2 r^2 - 2\beta\gamma r \tanh(\beta r)\right]$$

Evaluating therefore gives

$$\partial_r^2 h(0) = \beta^3 \gamma^{-1} \exp\left(-\gamma/2\right) \sqrt{\frac{2}{\pi\gamma}} \left(\gamma - 1\right).$$

So h is concave down whenever $\gamma < 1$ and concave up whenever $\gamma > 1$. ✓

A moment for γ (I) Return

Why does

$$h(r) = \frac{2}{\sqrt{2\pi\sigma^2}} \exp\left(\frac{-\mu^2 - r^2}{2\sigma^2}\right) \cosh\left(\frac{\mu r}{\sigma^2}\right),$$

lead to

$$M_{+1}M_{-1} = \frac{\pi}{2} \frac{1+\gamma}{[e^{-\gamma/2} + \sqrt{\pi\gamma/2}\mathrm{Erf}(\sqrt{\gamma/2})]^2}?$$

A moment for γ (II) Return

Define

$$\mu_n := \int_0^\infty r^n h(r) dr$$

A moment for γ (III) Return

By computation, and using $\gamma := \mu^2/\sigma^2$ and $\beta := \mu/\sigma^2$,

$$\mu_0 = 1$$

$$\mu_1 = e^{-\gamma/2}\sqrt{\frac{2\gamma}{\pi}}\frac{1}{\beta} + \frac{\gamma}{\beta}\mathrm{Erf}\left(\sqrt{\frac{\gamma}{2}}\right)$$

$$\mu_2 = \frac{\gamma^2+\gamma}{\beta^2}$$

A moment for γ (IV) Return

Notice!

- $h(r)$ is a distribution on the interval $(0, \infty)$.
- However, our data comes from a sample of a 2D space.

A moment for γ (V) Return

So the "true" distribution we are sampling is closer to

$$H(x,y) := \frac{h\left(\sqrt{x^2+y^2}\right)}{2\pi\mu_1},$$

since it has the correct radial behavior, is rotationally symmetric, and is properly normalized on the plane.

A moment for γ (VI) Return

So the moments we are numerically observing are

$$\begin{aligned} M_n &= \int\int H(x,y)\left(\sqrt{x^2+y^2}\right)^n dxdy \\ &= \int\int r^n \frac{h(r)}{2\pi\mu_1} rdrd\theta \\ &= \frac{\mu_{n+1}}{\mu_1} \end{aligned}$$

A moment for γ (VII) Return

By earlier computation,

$$M_{-1} = \frac{\mu_0}{\mu_1} = \frac{\beta}{e^{-\gamma/2}\sqrt{\frac{2\gamma}{\pi}} + \gamma \mathrm{Erf}\left(\sqrt{\frac{\gamma}{2}}\right)}$$

$$M_{+1} = \frac{\mu_2}{\mu_1} = \frac{(\gamma^2 + \gamma)/\beta}{e^{-\gamma/2}\sqrt{\frac{2\gamma}{\pi}} + \gamma \mathrm{Erf}\left(\sqrt{\frac{\gamma}{2}}\right)}$$

A moment for γ (VIII) Return

So, we directly get

$$M_{+1}M_{-1} = \frac{\pi}{2}\frac{1+\gamma}{[e^{-\gamma/2} + \sqrt{\pi\gamma/2}\mathrm{Erf}(\sqrt{\gamma/2})]^2}.\checkmark$$

Measuring $M_{+1}M_{-1}$? (I) Return

How do we measure $M_{+1}M_{-1}$?

Measuring $M_{+1}M_{-1}$? (II) Return

Estimate individual moments from numerically obtained values of

$$P_j(t) = x_j(t) + iy_j(t) := \sum_{k=1}^{N} J_{jk} \left(\cos(\theta_k(t)) + i \sin(\theta_k(t))\right),$$

by averaging over all N feilds and over the sampling window T.

$$M_{+1} \approx \frac{1}{NT} \sum_{j=1}^{N} \sum_{t=1}^{T} \sqrt{x_j(t)^2 + y_j(t)^2}$$

$$M_{-1} \approx \frac{1}{NT} \sum_{j=1}^{N} \sum_{t=1}^{T} \sqrt{x_j(t)^2 + y_j(t)^2}^{-1}$$

Measuring $M_{+1}M_{-1}$? (III) Return

We then estimate their product by averaging these moments across L independent simulations,

$$E[M_{+1}] = \mu_{+1} \approx \frac{1}{L}\sum_{l=1}^{L} M_{+1}^{(l)}$$

$$E[M_{-1}] = \mu_{-1} \approx \frac{1}{L}\sum_{l=1}^{L} M_{-1}^{(l)}$$

$$E[M_{+1}M_{-1}] \approx \frac{1}{L}\sum_{l=1}^{L} M_{+1}^{(l)}M_{+1}^{(l)}.$$

Note!

$$E[M_{+1}M_{-1}] \neq \mu_{+1}\mu_{-1},$$

because moments aren't independent.

Measuring $M_{+1}M_{-1}$? (IV) Return

Similarly,

$$\mathrm{Var}\left(M_{+1}\right) = \sigma^2_{+1}$$
$$\mathrm{Var}\left(M_{-1}\right) = \sigma^2_{-1}$$

can be estimated by online methods, but

$$\mathrm{Var}\left(M_{+1}M_{-1}\right)$$

is more difficult.

Measuring $M_{+1}M_{-1}$? (V) Return

The error on the product is given by

$$\mathrm{Var}\left(M_{+1}M_{-1}\right) \approx \frac{1}{L}\left[\mu_{+1}^2\sigma_{-1}^2 + \mu_{-1}^2\sigma_{+1}^2 + 2\mu_{+1}\mu_{-1}\mathrm{Cov}\left(M_{+1}, M_{-1}\right)\right] + O\left(\frac{1}{L^2}\right).$$

so this gives us a numerical way to estimate $M_{+1}M_{-1}$. ✓

$M_{+1}M_{-1}$ monotone? (I) Return

How the heck is

$$M_{+1}M_{-1} = \frac{\pi}{2}\frac{1+\gamma}{[e^{-\gamma/2} + \sqrt{\pi\gamma/2}\mathrm{Erf}(\sqrt{\gamma/2})]^2}$$

montone in γ?

$M_{+1}M_{-1}$ monotone? (II) Return

Let's define

$$\frac{\pi}{2f(\gamma)^2} = \frac{\pi}{2}\frac{1+\gamma}{[e^{-\gamma/2}+\sqrt{\pi\gamma/2}\mathrm{Erf}(\sqrt{\gamma/2})]^2},$$

so this expression is monotone if f is monotone in γ.

$M_{+1}M_{-1}$ monotone? (III) Return

Is

$$f(\gamma) = \frac{e^{-\gamma/2} + \sqrt{\pi\gamma/2}\mathrm{Erf}(\sqrt{\gamma/2})}{\sqrt{1+\gamma}},$$

monotone?

$M_{+1}M_{-1}$ monotone? (IV) Return

Is

$$f'(\gamma) = \frac{\sqrt{\pi/(8\gamma)}}{(1+\gamma)^{3/2}}\left(\mathrm{Erf}\left(\sqrt{\frac{\gamma}{2}}\right) - \sqrt{\frac{2\gamma}{\pi}}e^{-\gamma/2}\right)$$

single signed?

$M_{+1}M_{-1}$ monotone? (V) Return

Notice!

$$\text{Erf}\left(\sqrt{\frac{\gamma}{2}}\right) = \int_0^{\sqrt{\gamma/2}} \frac{2}{\sqrt{\pi}} e^{-t^2} dt$$

$M_{+1}M_{-1}$ monotone? (VI) Return

Also notice!

$$\sqrt{\frac{\gamma}{2}}e^{-\gamma/2} = \int_0^{\sqrt{\gamma/2}} e^{-t^2} - 2t^2 e^{-t^2}\, dt$$

$M_{+1}M_{-1}$ monotone? (VII) Return

Therefore!

$$f'(\gamma) = \frac{\sqrt{\pi/(8\gamma)}}{(1+\gamma)^{3/2}} \left(\int_0^{\sqrt{\gamma/2}} \frac{2}{\sqrt{\pi}} e^{-t^2} dt - \frac{2}{\sqrt{\pi}} \int_0^{\sqrt{\gamma/2}} e^{-t^2} - 2t^2 e^{-t^2} dt \right)$$

$M_{+1}M_{-1}$ monotone? (VIII) Return

Therefore!

$$\begin{aligned} f'(\gamma) =& \frac{\sqrt{\pi/(8\gamma)}}{(1+\gamma)^{3/2}} \int_0^{\sqrt{\gamma/2}} \frac{4}{\sqrt{\pi}} t^2 e^{-t^2} dt \\ \geq& 0. \end{aligned}$$

So $M_{+1}M_{-1}$ is monotone in γ! ✓

$M_{+1}M_{-1}$ monotone? (IX) Return

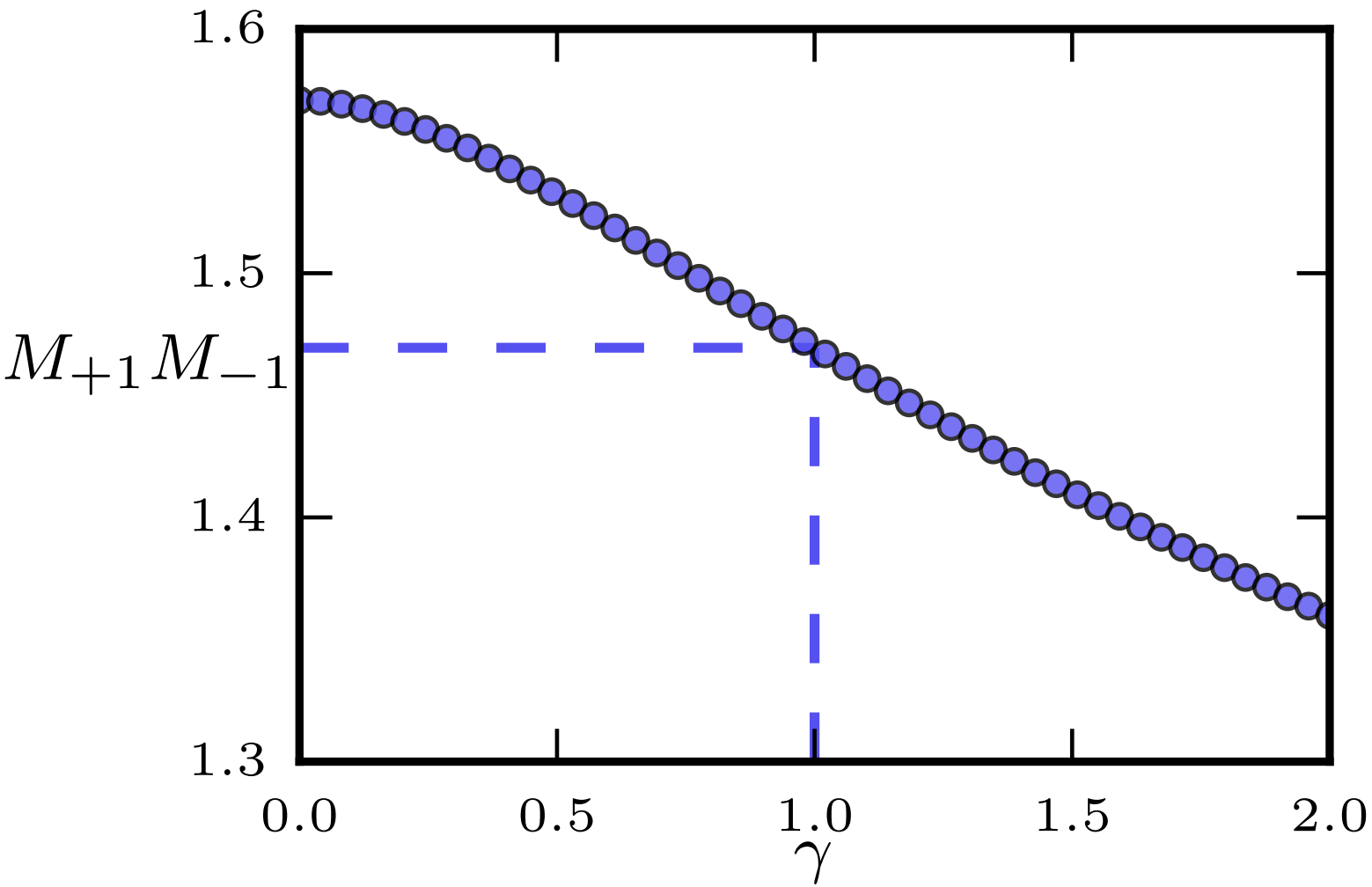

Appendix X 2 combo! (I) Return

Split the sum in half to get

$$\begin{aligned}\text{Term 2} =& 2\sum_{w=0}^{K-1}(K-1-2w)\binom{K-1}{w} \\ =& 2\sum_{w=0}^{K/2-1}(K-1-2w)\binom{K-1}{w} \\ &+ 2\sum_{w=K/2}^{K-1}(K-1-2w)\binom{K-1}{w}.\end{aligned}$$

Appendix X 2 combo! (II) Return

Letting $s := K - 1 - w$ gives

$$\text{Term 2} = 2 \sum_{w=0}^{K/2-1} (K - 1 - 2w) \binom{K-1}{w} + 2 \sum_{s=K/2-1}^{0} (-K + 1 + s) \binom{K-1}{K-1-s}.$$

Appendix X 2 combo! (III) Return

Therefore,

$$\begin{aligned}\text{Term } 2 =& 2\sum_{w=0}^{K/2-1}(K-1-2w)\binom{K-1}{w} \\ & -2\sum_{s=0}^{K/2-1}(K-1-2s)\binom{K-1}{s} \\ =& 0.\end{aligned}$$

What does frustration look like? Return

Figure: Each dot represents a distinct $\theta_j(t)$ over time under using a coupled oscillator model, with zero natural frequencies and random ± 1 coupling strengths. Here, $N = 75$, and we used a fourth-order Runge-Kutta integration with a step size of 0.002 across 2000 recorded steps, and initial phases distributed as a normal about 0. Each frame represents 10 steps.

Daido's dynamics: $J = 4$ Return

Figure: Distribution of local fields. Each dot represents a distinct $P_j(t)$ over time under using Daido's setup, with normally distributed coupling strengths and natural frequencies. Here, $N = 500$, $J = 4$ and we used a fourth-order Runge-Kutta integration with a step size of 0.01, 3600 recorded steps, and uniformly random initial phases. Each frame represents 10 steps.

Daido's dynamics: $J = 4$ Return

Figure: Distribution of phases versus natural frequencies. Each dot represents a distinct $\theta_j(t)$ over time under using Daido's setup, with normally distributed coupling strengths and natural frequencies. Here, $N = 500$, $J = 4$ and we used a fourth-order Runge-Kutta integration with a step size of 0.01, 3600 recorded steps, and uniformly random initial phases. Each frame represents 10 steps.

Daido's dynamics: $J = 14$ Return

Figure: Distribution of local fields. Each dot represents a distinct $P_j(t)$ over time under using Daido's setup, with normally distributed coupling strengths and natural frequencies. Here, $N = 500$, $J = 14$ and we used a fourth-order Runge-Kutta integration with a step size of 0.01, 3600 recorded steps, and uniformly random initial phases. Each frame represents 10 steps.

Daido's dynamics: $J = 14$ Return

Figure: Distribution of phases versus natural frequencies. Each dot represents a distinct $\theta_j(t)$ over time under using Daido's setup, with normally distributed coupling strengths and natural frequencies. Here, $N = 500$, $J = 14$ and we used a fourth-order Runge-Kutta integration with a step size of 0.01, 3600 recorded steps, and uniformly random initial phases. Each frame represents 10 steps.

New dynamics: $J = 1$ Return

Figure: Distribution of local fields. Each dot represents a distinct $P_j(t)$ over time under using our setup, with an interaction-vector based coupling and Cauchy distributed natural frequencies. Here, $N = 2500$, $K = 6$, $J = 1$ and using a fourth-order Runge-Kutta integration with a step size of 0.01, 3600 recorded steps, and uniformly random initial phases. Each frame represents 100 steps.

New dynamics: $J = 1$ Return

Figure: Distribution of semi-fields. Each dot represents a distinct $F_m(t)$ over time under using our setup, with an interaction-vector based coupling and Cauchy distributed natural frequencies. Here, $N = 2500$, $K = 6$, $J = 1$ and using a fourth-order Runge-Kutta integration with a step size of 0.01, 3600 recorded steps, and uniformly random initial phases. Each frame represents 100 steps.

New dynamics: $J = 1$ Return

Figure: Distribution of phases versus natural frequencies. Each dot represents a distinct $\theta_j(t)$ over time under using our setup, with an interaction-vector based coupling and Cauchy distributed natural frequencies. Here, $N = 2500$, $K = 6$, $J = 1$ and using a fourth-order Runge-Kutta integration with a step size of 0.01, 3600 recorded steps, and uniformly random initial phases. Each frame represents 100 steps.

New dynamics: $J = 1$ Return

Figure: Density of phase offsets from local fields versus coupling strength across all pairs of oscillators j and k. Darker cells correspond to higher densities. This simulation used our setup with an interaction-vector based coupling and Cauchy distributed natural frequencies. Here, $N = 2500$, $K = 6$, $J = 1$ and using a fourth-order Runge-Kutta integration with a step size of 0.01, 3600 recorded steps, and uniformly random initial phases. Each frame represents 100 steps.

New dynamics: $J = 1$ Return

Figure: Distribution of local fields and semi-fields. Each dot represents a distinct $P_j(t)$ or F_m over time under using our setup, with an interaction-vector based coupling and Cauchy distributed natural frequencies. Here, $N = 2500$, $K = 6$, $J = 1$ and using a fourth-order Runge-Kutta integration with a step size of 0.01, 3600 recorded steps, and uniformly random initial phases. Each frame represents 100 steps.

New dynamics: $J = 1$ Return

Figure: Distribution of phases versus natural frequencies. This simulation used our setup with an interaction-vector based coupling and Cauchy distributed natural frequencies. Here, $N = 2500$, $K = 6$, $J = 1$ and using a fourth-order Runge-Kutta integration with a step size of 0.01, 3600 recorded steps, and uniformly random initial phases. Each frame represents 100 steps.

New dynamics: $J = 1$ Return

Figure: Combination of all other videos. This simulation used our setup with an interaction-vector based coupling and Cauchy distributed natural frequencies. Here, $N = 2500$, $K = 6$, $J = 1$ and using a fourth-order Runge-Kutta integration with a step size of 0.01, 3600 recorded steps, and uniformly random initial phases. Each frame represents 100 steps.

New dynamics: $J = 3$ Return

Figure: Distribution of local fields. Each dot represents a distinct $P_j(t)$ over time under using our setup, with an interaction-vector based coupling and Cauchy distributed natural frequencies. Here, $N = 2500$, $K = 6$, $J = 3$ and using a fourth-order Runge-Kutta integration with a step size of 0.01, 3600 recorded steps, and uniformly random initial phases. Each frame represents 100 steps.

New dynamics: $J = 3$ Return

Figure: Distribution of semi-fields. Each dot represents a distinct $F_m(t)$ over time under using our setup, with an interaction-vector based coupling and Cauchy distributed natural frequencies. Here, $N = 2500$, $K = 6$, $J = 3$ and using a fourth-order Runge-Kutta integration with a step size of 0.01, 3600 recorded steps, and uniformly random initial phases. Each frame represents 100 steps.

New dynamics: $J = 3$ Return

Figure: Distribution of phases versus natural frequencies. Each dot represents a distinct $\theta_j(t)$ over time under using our setup, with an interaction-vector based coupling and Cauchy distirbuted natural frequencies. Here, $N = 2500$, $K = 6$, $J = 3$ and using a fourth-order Runge-Kutta integration with a step size of 0.01, 3600 recorded steps, and uniformly random initial phases. Each frame represents 100 steps.

New dynamics: $J = 3$ Return

Figure: Density of phase offsets from local fields versus coupling strength across all pairs of oscillators j and k. Darker cells correspond to higher densities. This simulation used our setup with an interaction-vector based coupling and Cauchy distributed natural frequencies. Here, $N = 2500$, $K = 6$, $J = 3$ and using a fourth-order Runge-Kutta integration with a step size of 0.01, 3600 recorded steps, and uniformly random initial phases. Each frame represents 100 steps.

New dynamics: $J = 3$ Return

Figure: Distribution of local fields and semi-fields. Each dot represents a distinct $P_j(t)$ or $F_m(t)$ over time under using our setup, with an interaction-vector based coupling and Cauchy distributed natural frequencies. Here, $N = 2500$, $K = 6$, $J = 3$ and using a fourth-order Runge-Kutta integration with a step size of 0.01, 3600 recorded steps, and uniformly random initial phases. Each frame represents 100 steps.

New dynamics: $J = 3$ Return

Figure: Distribution of phases versus natural frequencies. This simulation used our setup with an interaction-vector based coupling and Cauchy distributed natural frequencies. Here, $N = 2500$, $K = 6$, $J = 3$ and using a fourth-order Runge-Kutta integration with a step size of 0.01, 3600 recorded steps, and uniformly random initial phases. Each frame represents 100 steps.

New dynamics: $J = 3$ Return

Figure: Combination of all other videos. This simulation used our setup with an interaction-vector based coupling and Cauchy distributed natural frequencies. Here, $N = 2500$, $K = 6$, $J = 3$ and using a fourth-order Runge-Kutta integration with a step size of 0.01, 3600 recorded steps, and uniformly random initial phases. Each frame represents 100 steps.

Figure: Radial distribution of local fields. Each curve represents the averaged density over 500 simulations of Eq. (1), using $N = 250$, $K = 4$, fourth-order Runge-Kutta integration with a step size of 0.01, 1000 transient steps, 2000 recorded steps, and uniformly random initial phases.

Figure: Radial distribution of local fields. Each curve represents the averaged density over 500 simulations of Eq. (1), using $N = 250$, $K = 4$, fourth-order Runge-Kutta integration with a step size of 0.01, 1000 transient steps, 2000 recorded steps, and uniformly random initial phases.

Figure: Oscillator phase distributions below and above the volcano transition. In (a), $J = 1$; in (b), $J = 3$. Each panel shows results for simulations of $N = 2000$ and $K = 6$; other parameters as in Fig. 35. (a) Below the volcano transition, the system is incoherent. (b) Above the volcano transition, phase-locked clusters appear.

Convegrence to $J_C = 2$ Return

Figure: Critical value J_c versus N and K. Each value of J_c was estimated by using a bisection method on the value of $M_{+1}M_{-1}$ to achieve an accuracy of $\lesssim 0.02$. For each J we sample J_{jk} at least 100 times, simulate Eq. (1), evaluate $M_{+1}M_{-1}$, and keep track of the running standard deviation of these products. If the current value of $M_{+1}M_{-1}$ is more than 1.5 standard deviations from 1.4694, the bisection continues; otherwise further simulations are run, up to a maximum of 10^5 simulations. Each simulation consists of 1000 transient steps followed by 2000 recorded steps of a fourth-order Runge Kutta integration with a step size of 0.01, with initial phases all set to 0.

Algebraic decay? Return

Figure: Log-log plot for the decay of the order parameter $Z(t)$. Each curve is the average of 750 numerical integrations of Eq. (1) for $N = 5000$ oscillators starting from the in-phase state ($\theta_j = 0$ for all j) and run for 1000 steps with a step size of 0.01. Solid curves show coupled systems with $J = 10$; dashed curves show uncoupled systems with $J = 0$ for which the order parameter decays exponentially: $Z(t) = e^{-t}$. Simulation ran in the low-rank regime: $K \ll \log_2(N)$. For $K = 2$, $Z(t)$ decays exponentially down to the noise floor. Exponential decay is expected in this regime because the dynamics of Eq. (1) are well approximated by the low-dimensional system (4).

Algebraic decay? Return

Figure: Log-log plot for the decay of the order parameter $Z(t)$. Each curve is the average of 750 numerical integrations of Eq. (1) for $N = 5000$ oscillators starting from the in-phase state ($\theta_j = 0$ for all j) and run for 1000 steps with a step size of 0.01. Solid curves show coupled systems with $J = 10$; dashed curves show uncoupled systems with $J = 0$ for which the order parameter decays exponentially: $Z(t) = e^{-t}$. (a) Low-rank regime: $K \ll \log_2(N)$. For $K = 2$, $Z(t)$ decays exponentially down to the noise floor. Exponential decay is expected in this regime because the dynamics of Eq. (1) are well approximated by the low-dimensional system (4). (b) High-rank regime: $K = N = 5000$. When $K = O(N)$ and $J > J_c$, the relaxation of Z slows markedly, resembling the algebraic decay in glass.

Algebraic decay? Return

Figure: Log-log plot for the decay of the order parameter $Z(t)$. Each curve is the average of 750 numerical integrations of Eq. (1) for $N = 5000$ oscillators starting from the in-phase state ($\theta_j = 0$ for all j) and run for 1000 steps with a step size of 0.01. Solid curves show coupled systems with $J = 10$; dashed curves show uncoupled systems with $J = 0$ for which the order parameter decays exponentially: $Z(t) = e^{-t}$. (a) Low-rank regime: $K \ll \log_2(N)$. For $K = 2$, $Z(t)$ decays exponentially down to the noise floor. Exponential decay is expected in this regime because the dynamics of Eq. (1) are well approximated by the low-dimensional system (4). (b) High-rank regime: $K = N = 5000$. When $K = O(N)$ and $J > J_c$, the relaxation of Z slows markedly, resembling the algebraic decay in glass.